Universidade de Aveiro Departamento de Química
2017

GONÇALO VIEIRA SARAIVA DE OLIVEIRA

REMOÇÃO DE FÁRMACOS DA ÁGUA USANDO ADSORVENTES PRODUZIDOS A PARTIR DA PASTA DE PAPEL

REMOVAL OF PHARMACEUTICALS FROM WATER USING PAPER PULP-BASED CARBON ADSORBENTS

Universidade de Aveiro Departamento de Química
2017

GONÇALO VIEIRA SARAIVA DE OLIVEIRA

REMOÇÃO DE FÁRMACOS DA ÁGUA USANDO ADSORVENTES PRODUZIDOS A PARTIR DA PASTA DE PAPEL

REMOVAL OF PHARMACEUTICALS FROM WATER USING PAPER PULP-BASED CARBON ADSORBENTS

Dissertação apresentada à Universidade de Aveiro para cumprimento dos requisitos necessários à obtenção do grau de Mestre em Biotecnologia Industrial e Ambiental, realizada sob a orientação científica da Doutora Vânia Maria Amaro Calisto, Estagiária de Pós-doutoramento do Departamento de Química da Universidade de Aveiro, e do Doutor Valdemar Inocêncio Esteves, Professor Auxiliar do Departamento de Química da Universidade de Aveiro.

Cofinanciado por:
COMPETE 2020 PROGRAMA OPERACIONAL COMPETITIVIDADE E INTERNACIONALIZAÇÃO
PORTUGAL 2020
UNIÃO EUROPEIA Fundo Europeu de Desenvolvimento Regional
FCT Fundação para a Ciência e a Tecnologia
MINISTÉRIO DA CIÊNCIA, TECNOLOGIA E ENSINO SUPERIOR

Apoio financeiro da FCT e COMPETE2020 no âmbito do projeto de investigação PTDC/AAG-TEC/1762/2014

o júri

presidente

Professor Doutor João Manuel da Costa e Araújo Pereira Coutinho
Professor Catedrático da Universidade de Aveiro

Doutora Marta Otero Cabero
Equiparada a Investigadora Principal no Departamento do Ambiente e Ordenamento da Universidade de Aveiro

Doutora Vânia Maria Amaro Calisto
Estagiária de Pós-Doutoramento no Departamento de Química da Universidade de Aveiro

agradecimentos

À minha família, por todo o apoio prestado durante o tempo dedicado na realização deste trabalho.

À minha orientadora, Vânia Calisto, pela orientação científica, pelas sugestões e críticas construtivas e por, acima de tudo, se mostrar sempre disponível, desde o primeiro dia em que me apresentou o laboratório e me convenceu definitivamente a aceitar este projeto.

Ao Professor Valdemar Esteves e às minhas colegas de laboratório, por toda a ajuda e total disponibilidade.

À Eng.ª Maria Miguel (Luságua) pela cedência dos efluentes.

A todos os meus amigos, pelos momentos de descontração também necessários nesta etapa e pela contagiante boa disposição, que me ajudou a superar os dias mais complicados.

E por fim mas não menos importante, à Ana Guerrinha, por me ter apoiado sempre, incondicionalmente, por estar comigo desde o início e por, imensas vezes, ter esperado horas, só por causa de uns minutos. Minutos esses que compensavam um dia inteiro de trabalho. Foi ela que me deu a força e motivação necessárias para ultrapassar os momentos mais difíceis e por isso mesmo agradeço-lhe mais do que tudo.

palavras-chave

Adsorção; Carvões Ativados; Fármacos; Tratamento de água; Sustentabilidade; Isotérmicas de adsorção; Pasta crua; Pasta branqueada; Indústria do papel

resumo

A existência de fármacos no meio ambiente, em particular ambientes aquáticos, constitui um problema preocupante, sendo as Estações de Tratamento de Águas Residuais (ETAR) a principal via de entrada destes compostos no meio, devido à sua ineficácia para os remover das águas contaminadas. A adsorção é um método bastante eficiente, sendo os carvões ativados os adsorventes mais comummente utilizados. Uma vez que os carvões ativados comerciais são caros, em parte devido ao preço dos seus precursores, a produção de adsorventes a partir de matérias-primas alternativas é uma solução interessante que se enquadra no conceito de economia sustentável. Neste trabalho foram utilizados dois tipos de pasta, branqueada (BP) e crua (RP), derivadas do processo de produção da pasta de papel, como precursores para a produção de carvões ativados e não ativados. Na ativação, as pastas foram impregnadas com dois agentes químicos ativantes (K_2CO_3 ou H_3PO_4) e posteriormente pirolisadas e lavadas com ácido. Após a produção, os materiais foram física e quimicamente caraterizados. De forma a testar o desempenho dos carvões enquanto adsorventes, foram realizados testes de adsorção em descontínuo com água ultrapura e com efluentes recolhidos em ETAR, utilizando dois fármacos: o antiepilético carbamazepina (CBZ) e o antibiótico sulfametoxazol (SMX). Para as quantidades de carvão utilizadas, os resultados em água-ultrapura mostraram adsorção nula para os carvões não ativados e boas capacidades de adsorção para os carvões ativados. Comparando os testes realizados para os efluentes reais com CBZ e SMX, os testes com SMX apresentaram baixas capacidades de adsorção, provavelmente devido às diferentes interações estabelecidas entre as superfícies do fármaco e do carvão, na presença de elevada carga orgânica. Os testes com efluentes reais apresentaram melhores capacidades de adsorção para carvões ativados com H_3PO_4 e produzidos a partir da BP: 92 ± 19 $mg.g^{-1}$ para a CBZ e 13.0 ± 0.6 $mg.g^{-1}$ para o SMX. Estes resultados refletem as potencialidades destas pastas para serem utilizadas como precursoras de carvões ativados, os quais podem ser aplicados no tratamento de águas residuais.

keywords

Adsorption; Activated carbons; Imerging contaminants; Water treatment; Sustainability; Adsorption isotherms; Raw pulp; Bleached pulp; Paper industry

abstract

The occurrence of pharmaceuticals in the environment, mainly aquatic, is a worrying issue, with Wastewater Treatment Plants (WWTP) being the main entry route of these compounds due to their inefficient ability to remove them from contaminated water. Adsorption is a very effective method for this purpose, with activated carbons being the most commonly used adsorbents. Considering that commercial activated carbons are expensive, in part due to the price of their precursors, the production of adsorbents from alternative raw materials is an interesting solution and fits within the concept of sustainable economy. In this work, two type of pulps, bleached (BP) and raw pulp (RP), derived from the pulp and paper production process, were used as precursors for production of non-activated and activated carbons. For activated carbons, the pulps were impregnated with two chemical activating agents (K_2CO_3 or H_3PO_4), and then pyrolysed and washed with acid. After production, the materials were physically and chemically characterized. To test the performance of these carbons as adsorbents, batch adsorption tests were performed with ultra-pure water and with WWTP effluents, using two pharmaceuticals: the anti-epileptic carbamazepine (CBZ) and the antibiotic sulfamethoxazole (SMX). For the amounts of carbon tested, in ultra-pure water, the results showed no adsorption for non-activated carbons and good adsorption capacities for the activated ones. Comparing the adsorption tests in real effluents with CBZ and SMX, tests with SMX presented low adsorption capacities, probably due to the different interactions establish between the two pharmaceuticals and carbons surface, in the presence of high organic load. Tests with real effluents presented better adsorption capacities for carbons activated with H_3PO_4 and produced from BP: 92 ± 19 mg g^{-1} for CBZ and 13.0 ± 0.6 mg g^{-1} for SMX. These results indicate the potential of these pulps to be used as precursors for activated carbons that can be applied in wastewater treatment.

Contents

List of figures

List of tables

Abbreviations

ATR – Attenuated total reflectance

ASS – Absolute sum-of-squares

BET – Brunauer, Emmett and Teller

BP – Bleached pulp

CBZ – Carbamazepine

CZE – Capillary zone electrophoresis

$\boldsymbol{D}$ – Average pore diameter

DOC – Dissolved organic carbon

EKC – Electrokinetic capillary chromatography

EOF – Electroosmotic flow

FC – Fixed carbon

FTIR – Fourier transform infrared spectroscopy

GAC – Granular activated carbons

HPLC – High performance liquid chromatography

IC – Inorganic carbon

LOD – Limit of detection

LOQ – Limit of quantification

MEKC – Micellar electrokinetic chromatography

PAC – Powder activated carbons

PZC – Point of zero charge

RP – Raw pulp

$\boldsymbol{S_{BET}}$ – Specific surface area

SDS – Sodium dodecyl sulphate

SEM – Scanning electron microscopy

TC – Total carbon

TGA – Thermogravimetric analysis

TOC – Total organic carbon

VM – Volatile matter

$\boldsymbol{V_p}$ – Total pore volume

$\boldsymbol{W_0}$ – Total micropore volume

WWTP – Wastewater treatment plant

I. Introduction

1) Removal of pharmaceuticals from water by adsorption

1.1) Occurrence of pharmaceuticals in the environment

The use of pharmaceuticals has been increasing considerably over time and with this, their concentration in the environment, mainly in aquatic environments, has grown up too, reaching the levels of microgram per liter [1]. Actually, despite many studies have been published in the last few years about organic pollutants and their effects in the environment, they reveal a scarce and incomplete knowledge which do not allow a full and accurate assessment of all risks associated with the disposal of these contaminants in the environment [2, 3].

In fact, the main pathway for the entrance of pharmaceutical drugs into the environment is the discharge of effluents from Wastewater Treatment Plants (WWTP). There is a limited capacity to remove pharmaceutical products from urban wastewaters because microorganisms cannot metabolize most drugs as source of carbon [4–7]. In Table 1 it is schematized the concentration of various drugs before and after treatment on WWTP's. Due to their physical and chemical properties, pharmaceutical drugs have different behaviours when subjected to water treatments and, although some treatments are efficient and can remove these compounds from water, most of them are not effective [1]. It is the case of WWTP, which are very inefficient in removing drugs from water and are responsible for the release of water still contaminated in the aquatic resources that ultimately supply the population.

Table 1 - Drug concentrations detected in wastewaters before and after treatment on WWTP's. Adapted from Rivera-Utrilla et al. (2013) [4]

Type of pharmaceutical	Substance detected	WWTP inlet ($ng\,L^{-1}$)	WWTP outlet ($ng\,L^{-1}$)
Analgesics and anti-inflammatories	Ketoprofen	451	318
	Naproxen	99	108
	Ibuprofen	516	266
	Diclofenac	250	215
	Acetaminophen	10 194	2102
Lipid-lowering drugs	Bezafibrate	23	10
	Clofibrate	72	28
	Gemfibrozil	155	120
Antiepileptics	Carbamazepine	420	410
Antacids	Ranitidine	188	135
Antibiotics	Azithromycin	152	96
	Metronidazole	80	43
	Sulfamethoxazole	590	390
	Trimethoprim	1172	290
β-Blockers	Atenolol	400	395
	Sotalol	185	167
	Propanolol	290	168

This fact has been worrying the scientific community, which caused the search for new solutions to try to solve this serious environmental problem. One of the proposed solutions is based on the adsorption of pollutants onto adsorbent materials. This technique is based on the use of adsorbents that have the ability to remove pollutants from water, most commonly activated carbons,

making the purification process possible. It is a very versatile and efficient solution to remove contaminants from the environment [8]. This technology may involve batch or continuous processes, as described in Ali et al. (2007) [9].

1.2) Adsorption

Adsorption process occurs when a solid surface is exposed to gas or liquid and there is an enrichment of material on the adsorbent surface or an increase of the fluid density in the vicinity of an interface [10]. The increase of this specific component concentration is dependent on the extension of interfacial area. That is why adsorbents used at industrial level have a large specific surface area and are quite porous.

Adsorption may be of two types, depending on the nature of the forces involved: physical adsorption and chemisorption. In the first case, adsorbate is bound to the surface by relatively weak van der Walls forces. Chemisorption involves exchange or sharing of electrons between the adsorbate molecules and the surface of the adsorbent, resulting in a chemical reaction. The formed covalent bond is much stronger than the physical adsorption bond. The magnitude of the enthalpy of adsorption is the most important difference between the two types of adsorption: in physical adsorption, the enthalpy of adsorption does not usually exceed 10 to 20 KJ per mol, whereas in chemisorption the enthalpy is generally of the order of 40 to 400 KJ per mol. Physical adsorption is nonspecific and occurs between any adsorbate-adsorbent systems. Contrariwise, chemisorption is specific. The type of the adsorption that takes place in a system depends on the nature of the adsorbate, the nature of the adsorbent, the reactivity of the surface, the surface area of the adsorbate, and the temperature and pressure of adsorption [8].

The adsorption rate of a given material depends on the physical and chemical properties of adsorbent and on the material to be adsorbed (adsorbate), essentially on the adsorbent pore size and molecular weight and configuration of the adsorbate [11]. Also, the surface chemistry of the adsorbent proves to be a fundamental aspect for the occurrence or not of an efficient adsorption. For example, in dilute aqueous solutions, the chemical properties of the adsorbent are decisive for the occurrence of electrostatic and non-electrostatic interactions that influence the adsorption mechanism [12]. From a more general point of view, the adsorption capacity depends essentially on the accessibility of adsorbate molecules to the surface of the adsorbent. Beyond these factors, in some systems, the adsorption rate also depends on external factors as pH, ionic strength and temperature [11].

Both adsorption of gas molecules and adsorption of molecules in solution are described by the same process: when a gas or solution is exposed to a solid surface, gas molecules or solutes begin to be adsorbed onto that surface, occurring at a high adsorption rate. As surface pores begin to be

filled, adsorption rate decreases and the reverse process - desorption - begins to occur. When adsorption rate equals desorption rate, the adsorption equilibrium is reached, which corresponds to the maximum value of adsorbed molecules onto the adsorbent [8]. Although the adsorption process can refer to the adsorption of molecules present in solutions or gases, only adsorption of solutes will be addressed, since the objective of the work, as explained later, consists of removing drugs from contaminated waters.

Apart from the solute, some amount of solvent may also be adsorbed onto the solid surface, in the case of a liquid-solid adsorption system. Considering that only solute adsorption takes place, the amount of adsorbed solute after a certain time, q_t (mg g^{-1}), can be defined by Equation 1:

$$q_t = \frac{(C_0 - C_t)V}{m}$$

Equation 1

where C_0 and C_t refer to solute concentrations in solution at the beginning of the process and after a certain time t, respectively (mg L^{-1}), V refers to the volume of solution used (L) and m refers to the mass of adsorbent used (g) [12].

In most adsorption studies reported in the literature, applied to the removal of environmental pollutants, the solute concentration used is usually about 20 000 times higher than the concentration found in the environment: for example 5 mg L^{-1} of carbamazepine (CBZ) was used in Calisto et al. (2015) [13] comparing to 248 ng L^{-1}, the average concentration of CBZ found in 122 samples of European rivers [14]. It is experimentally challenging to use environmentally relevant concentrations of solute because it would imply the use of very low adsorbent mass concentrations to obtain a good kinetic and equilibrium profile, and the use of very sensitive analytical techniques, which are quite costly and time consuming. For this reason, the initial drug concentration used in the performed adsorptive experiments of this work was 5 mg L^{-1}.

1.3) Adsorption isotherms

When studying the adsorption potential of a material to remove a certain contaminant it is necessary to evaluate its performance and the maximum capacity of adsorption under equilibrium conditions. For this, it is necessary to determine the associated adsorption isotherms. An adsorption isotherm is a function that describes the retention of a solute from the aqueous phase onto the solid adsorbent phase at constant pH and constant temperature, varying the solute concentration using a fixed adsorbent concentration, or varying the adsorbent concentration with a fixed solute concentration [15]. This parameter evaluates the adsorbents capacity to adsorb a certain solute and

represents the first information to be used on choosing one adsorbent over another for the solute in question. The liquid-solid adsorption equilibrium is obtained when the adsorbate in solution remains enough time in contact with the adsorbent so that there is a balance between adsorbate concentration on aqueous phase and adsorbate concentration on adsorbent interface. It is this equilibrium that is expressed mathematically and plotted in a graph, giving rise to several types of isotherms [8, 12]. Adsorption isotherms also often refer to the adsorption of gas molecules onto adsorbents surface, which allows to determine the porosity of adsorbents and the determination of their specific surface area. This case is exemplified by the method developed by Brunauer, Emmett and Teller (1938) [16] which uses nitrogen adsorption isotherms to determine the specific surface area of adsorbents (S_{BET}). Despite less used, isotherms of a liquid-solid adsorption system can also be applied to determine the specific surface area, with the advantage that a vacuum system is not required, as in gas-solid adsorption systems, which makes this process faster [8,12].

There are several types of isotherms already studied by several authors. Four main groups can be identified: S (Sigmoid), C (Linear), H (High affinity) and L (Langmuir) [17]. There is also the type F (Freundlich) isotherm which is often considered to be an L-type derivative [8]. These isotherms are schematically shown in Figure 1:

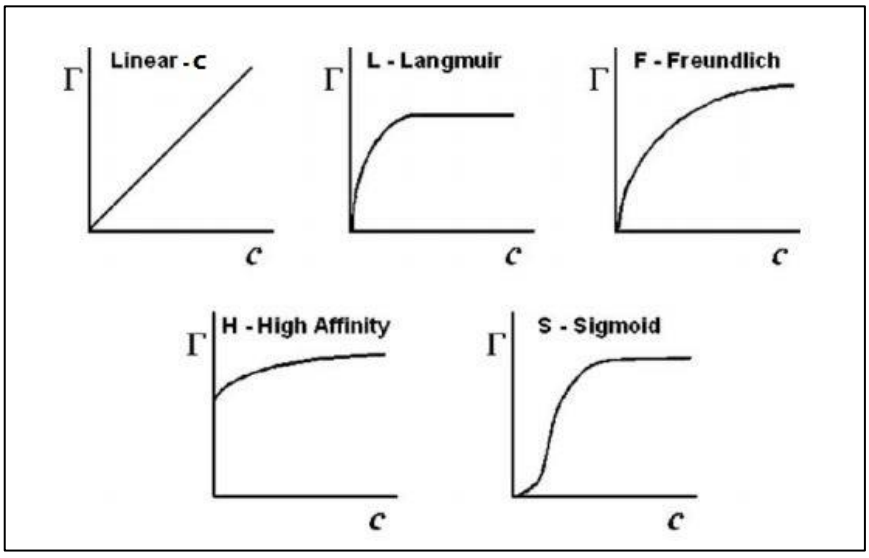

Figure 1 – Most common adsorption isotherms in liquid-solid systems. Adapted from Moreno-Castilla et al. (2004) [12]

L-curves are the most commonly observed and occur mostly in adsorption processes from dilute solutions [17]. In these curves and in later stages of H and S type curves, the more solute is transferred to the adsorbent surface, the less likely a solute molecule is able to find a binding site on adsorbent surface in order to be adsorbed. The solute molecule is considered non-vertically oriented

and there is no strong competition from the solvent. In contrast, in the first stage of the S curve, the initial binding of solute molecules to adsorbent surface enhances the binding of more molecules and the occurrence of a higher adsorption rate. This mechanism is called cooperative adsorption [17].

In C curves, the availability of possible surface sites to bind a solute remains constant over time, even with the increase of solute concentration. This linearity means that as new solute molecules bind, new binding sites are formed on the adsorbent surface. This happens when the solute has more affinity for the substrate present on the adsorbent surface than the solvent itself, which causes the creation of new interfacial spaces by the solute molecules that penetrate the surface and remain there retained [17].

Type H curves are a special case of type L curves, where solute molecules have such a affinity for the adsorbent used that the initial phase of the curve is vertical, which corresponds to an immediate adsorption of molecules by the adsorbent.

There are several mathematical models that allow the interpretation of adsorption isotherms, more specifically the behaviour of solute molecules in relation to the used adsorbent and the established interactions. Some examples are the Langmuir, Freundlich and Langmuir-Freundlich mathematical models.

1.3.1) Langmuir isotherm model

The Langmuir isotherm model [18] considers that adsorption occurs at homogeneous sites on the adsorbent surface and that the maximum adsorption reached corresponds to the saturation with a monolayer of the solute molecules on the adsorbent surface. In order to consider that an adsorption process follows this model, the next assumptions must be made: the adsorption process takes place in a monolayer where its thickness corresponds to the length of a single molecule, occurs in a finite number of identical and equivalent sites located in well-defined spaces, there are no interactions between the adsorbed molecules and all the binding sites have the same affinity for the adsorbed molecules and are energetically equivalent, resulting in a homogeneous adsorption [8] [15].

Mathematically, this isotherm is defined by Equation 2:

$$q_e = \frac{q_m \times K_L \times C_e}{1 + K_L \times C_e}$$

Equation 2

where q_e corresponds to the amount of adsorbate at equilibrium (mg g^{-1}), q_m is the maximum adsorbed solute (mg g^{-1}), C_e refers to the concentration of adsorbed solute at equilibrium (mg L^{-1}) and K_L is the Langmuir equilibrium constant (L mg^{-1}). Another expression can be used to better define this type of

isotherm, namely the type of equilibrium reached, using the determination of the separation factor R_L [19]:

$$R_L = \frac{1}{1 + K_L \times C_0}$$

Equation 3

where C_0 is the initial solute concentration (mg L^{-1}). If:

- R_L=0: Irreversible adsorption
- 0 <R_L <1: Favourable adsorption
- R_L=1: Linear adsorption
- R_L> 1: Non-favourable adsorption

1.3.2) Freundlich isotherm model

This isotherm model [20] represents an empirical equation to describe heterogeneous systems. As the solute concentration increases, also the amount of adsorbate on adsorbent surface increases, with the absence of a well-defined equilibrium state, as in the Langmuir isotherm. This means that there is not a maximum adsorption capacity and it can only be used medium-low concentrations of solutes.

Unlike Langmuir model, the Freundlich model describes a reversible and non-ideal adsorption and can be applied to adsorptions in monolayer and multilayer [15]. Equation 4 describes this isotherm:

$$q_e = K_F \times Ce^{(1/n)}$$

Equation 4

where K_F is the Freundlich equilibrium constant (mg g^{-1} (L $mg^{-1})^{1/n}$) and n is the Freundlich constant related with the level of non-linearity of equation. It represents a measure of adsorptive intensity. If n<1, the adsorption is non-favourable, if n=1, linear, and if n>1, favourable [8].

1.3.3) Langmuir-Freundlich isotherm model

A new isotherm was suggested by Sips (1948), being a combined form of Langmuir and Freundlich expressions for predicting the heterogeneous adsorption systems allowing to solve the limitations of Freundlich isotherm model. Thus, at low adsorbate concentrations, it is equivalent to a Freundlich isotherm; at high concentrations, it predicts a monolayer adsorption capacity characteristic of the Langmuir isotherm. This isotherm is described by Equation 5:

$$q_e = \frac{q_{\max LF} \times K_{LF} Ce^{N_{LF}-1}}{1 + K_{LF} Ce^{N_{LF}-1}}$$

Equation 5

where q_{maxLF} (mg g^{-1}) represents the Langmuir-Freundlich maximum adsorption capacity, K_{LF} (mg g^{-1} (mg $L^{-1})^{-1/N_{LF}}$) is the affinity coefficient of Langmuir-Freundlich model and N_{LF} is the degree of non-linearity.

1.4) Adsorption kinetics

In addition to adsorption equilibrium, this process involves another inherent factor that is the adsorption kinetics. This includes the adsorption study of molecules present in solutions or gases over time. There are many models proposed in literature for these kinetics studies, such as the pseudo-first order [21] and pseudo-second order [22] models, Elovich's model [23] and the intraparticle diffusion model [11], being the most commonly used the pseudo-first and pseudo-second order models.

1.4.1) Pseudo-first order model

Lagergren (1898) [21] suggested this model to describe a case of liquid-solid adsorption. This model is the earliest known, where the adsorption capacity of the solute is evaluated. There is a direct proportional ratio between solute's rate of adsorption over an established time and the difference between adsorbate at equilibrium and adsorbate at this established time. This relation is defined by the following mathematical equation:

$$\frac{dq}{dt} = k_1(q_e - q_t)$$

Equation 6

where q_t is the quantity of adsorbate removed at time t per unit mass of adsorbent (mg g^{-1}), q_e refers to the amount of adsorbate per unit mass of adsorbent at equilibrium (mg g^{-1}) and k_1 is the pseudo-first order rate constant (min^{-1}).

1.4.2) Pseudo-second order model

Ho (2000) assigned a second-order model to a kinetic process of divalent metal ions adsorption, where the rate limiting step was chemical adsorption, involving valence forces through sharing or exchanging of electrons [22]. This model is also based on the adsorption capacity and can be applied to adsorption of metal ion and organic substances, as pharmaceuticals, dyes, pesticides and oils, from aqueous solutions. The pseudo-second order model is described by Equation 7:

$$\frac{dq}{dt} = k_2 (q_e - q_t)^2$$

Equation 7

where k_2 is the rate constant of pseudo-second order (g mg^{-1} min^{-1}).

Lagergren's first order and Ho's second order equations have been called pseudo-first and pseudo-second order with the purpose to distinguish a kinetic equation based on the adsorption capacity of a solid, from the ones based on the concentration of a solution.

1.5) Basic concepts of capillary electrophoresis

Kinetic and isothermal adsorption studies involve the quantification of adsorbate concentration in the aqueous phase. In this study, the quantification of pharmaceuticals was performed using the capillary electrophoresis technique [24]. The main concept of electrophoresis is based on the separation of charged molecules that move along a fluid after application of a constant electric field. Capillary electrophoresis uses a thin capillary as physical support for molecules separation. When compared to other separative techniques such as high performance liquid chromatography (HPLC), capillary electrophoresis has several advantages [24]:

- Requires a small amount of reagents and sample.
- Capillaries are less expensive than HPLC columns.
- Capillaries are more versatile because they allow the easy manipulation of their surface by applying of a coating or a (pseudo) stationary phase.
- It allows the separation of molecules with a larger range of molecular weights and charges.
- It has higher efficiency and separation resolution than HPLC.

The capillary electrophoresis process is outlined in Figure 2.

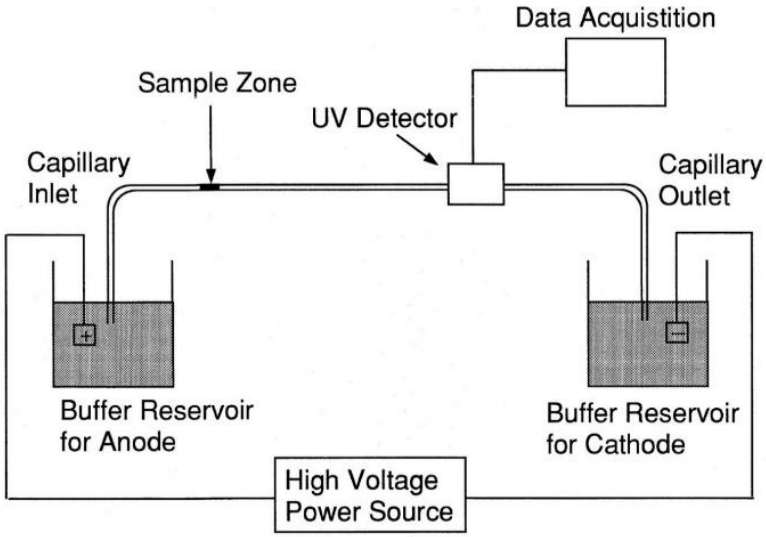

Figure 2 - Scheme of the capillary electrophoresis process [25]

Electrophoretic separation depends on electrophoretic mobility, electroosmotic flow (EOF) and on the different molecular weights and conformations of the analyte [24]. The electrophoretic mobility of charged molecules in an electrolytic solution is a consequence of the electrostatic force exerted when a constant electric field is applied. EOF is the liquid flow originated in the presence of an electric field and when an electrolyte solution comes in contact with the charged inner walls of the capillary.

The separation of charged molecules depends on their different electrophoretic mobilities as well as on electroosmotic flow, which is dependent on inner wall charge of the capillary. The separation happens after the capillary is filled with an electrolytic solution (buffer). After sample injection into the capillary, a constant electric field is applied between source and destination vials which initiates the migration of analytes along the capillary, from inlet to outlet. This separation mode is called capillary zone electrophoresis (CZE). Analytes can be detected near the outlet, through the absorbance in the UV or UV-visible zone, or using other detectors, such as fluorescence or mass spectrometry detection. After detection, an electropherogram is obtained, and the peaks area can be integrated and correlated with the analyte concentration in the sample.

The problem with this separation technique (CZE) is being limited to charged molecules. However, the separation of neutral molecules became possible with the development of electrokinetic capillary chromatography (EKC), which consists of introducing a pseudo-stationary phase in the separation buffer. In this case, the separation of neutral molecules is dictated by a partition between the pseudo-stationary and aqueous phases. The most common way of creating a pseudo-stationary phase is to use a surfactant to create micelles, which are spontaneously formed aggregates of surfactant molecules in aqueous solutions. This mode of separation is called micellar electrokinetic

chromatography (MEKC) and it consists of the partition of analytes between micelles and the aqueous phase. The most commonly used surfactant is sodium dodecyl sulphate (SDS) for having a large water solubility, degree of lipid solubilisation and a low critical micellar concentration (8 mM) [24]. A MEKC method was optimized in Calisto (2011) [24], where the results show that dynamically coated capillaries were advantageous to improve the reproducibility of analytes separation because they decrease the variability in the interactions between the analytes and the capillary inner wall. The procedure described in Calisto (2011) [24] consists of coating the capillary surface with polybrene, a multiple charged polycation, and then coating the positively charged surface with an anionic surfactant (SDS). As schematized in Figure 3, the first layer of SDS interacts with the cationic surface of polybrene and a second layer of SDS is formed by establishing hydrophobic interactions with the first one, resulting in a highly negatively charged surface.

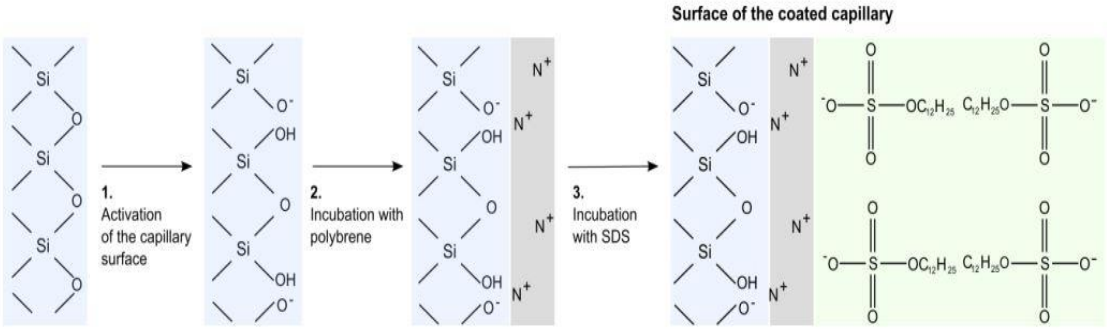

Figure 3 – Schematic representation of the capillary coating process [24]

2) Alternative adsorbents: a new approach

2.1) Production of carbons from alternative precursors

Commercial activated carbons are very efficient in adsorption processes. However, their production cost is high since the most common used raw materials are petroleum coke, a product obtained during the oil refining process, and charcoal. In addition to the high price, these precursors also originate environmental problems [26]. The production of adsorbent materials from low-cost alternative raw materials is an increasingly present reality. Given the global economic context and environmental problems such as the depletion of fossil resources and the increase of greenhouse effect, this solution is becoming more and more important in line with the need to adopt processes that promote a more sustainable economy. The production of adsorbents for water treatment is no exception and given this, adsorbents have been developed from cheap biological raw materials from diverse origins [27]. The most common type of produced adsorbents are carbon-based materials such as activated carbons. There are several works in scientific literature concerning the production of carbons adsorbents from various types of substrates. Agricultural residues are the most common type,

where adsorbents were produced from cocoa [28] and coconut [29] shells, cherry stones [30], potato peels [31], Isabel grape bagasse [32], coffee residues and almond shells [33], among many others. Adsorbents were also produced from industrial residues like macroalgae waste originated in Agar-Agar industry [34], carbon residues from woody biomass gasification [35], cellulose sludge [36] and sewage sludge of industrial laundries [37]. Many works have already been published comparing the use of commercial activated carbons with adsorbents produced from low cost raw materials [38–40] and many of them have shown better adsorption capacities than commercial activated carbons and better adsorption capacity/price ratio.

One type of substrate that has also been exploited to produce adsorbents is the resulting sludge from the pulp and paper industry [13, 40–45]. A 2009 study concluded that these residues were produced at a rate of eleven million tons per year in Europe alone [46]. Beyond the abundance of this raw material, it also presents very interesting characteristics for the production of adsorbents because they are lignocellulosic materials, which are good precursors for activated carbons due to high percentage of carbon and volatiles [47]. The three main components of these materials (cellulose, hemicellulose and lignin) contribute to the development of pores and micropores in the final carbon, characteristic of a good adsorbent.

In Calisto et al. (2014) [45], residual sludge from paper industry was used as substrate for the production of adsorbents to remove citalopram, an antidepressant drug, from water. Pyrolysis of primary and biological sludge from this industry originated highly aromatic carbons. The carbon specific surface area increased with the pyrolysis temperature and its residence time. In this work, it was concluded that pyrolysis of primary sludge at 800ºC for 150 minutes gave rise to carbons with higher adsorption capacity and the most interesting physicochemical characteristics: higher surface area and higher volume of pores and micropores [45].

In another work, Calisto et al. (2015) [13] tested the adsorption of seven different drugs using a commercial activated carbon and a non-activated carbon produced by pyrolysis of primary sludge resulting from paper industry, concluding that adsorption was greater on commercial activated carbon. However, the adsorption kinetics of low-cost carbon was rapid, reaching the equilibrium quickly [13]. This is an important fact because fast adsorption also represents an advantage to be taken into account in what concerns the real applicability of the process.

2.2) Activated carbons and their potential

Studies about the production of activated carbons with similar characteristics to commercial activated carbons have been carried out, since adsorbents produced with no activation have generally a weak performance [40], being necessary to activate their precursors to generate adsorbents with good efficiency.

Activated carbons have a large number of applications such as the adsorptive removal of undesirable organic and inorganic pollutants from drinking water and the purification of air, which results in the possibility of being used in food processing and chemical industries. They may also be used in medical applications for the adsorptive removal of toxins and poisons and purification of blood [8]. The application that is the focus of this work is the removal of pharmaceuticals from contaminated water.

The purpose of activation is the increase of pores number in the adsorbent's surface, increasing the specific surface area and in turn, expectedly, the adsorption capacity of the material. According to IUPAC classification, there are three main classes of pores, conforming to their diameter: micropores (<2 nm), mesopores (between 2 and 50 nm, inclusive) and macropores (> 50 nm). The choice of the activating agent used in the impregnation of the precursor material influences the pore distribution of the resulting material [48].

Activated carbons may be powder activated carbons (PAC) or granular activated carbons (GAC). PAC have a finer particle size with a maximum value of 180 μm. Above this value, activated carbons are considered to be granular. PAC allows faster adsorption and are generally used in batch conditions, being difficult to regenerate. GAC are very mechanically resistant, which allows to withstand the operating conditions, such as high pressures. They can be used in fixed adsorption beds and have the possibility of being regenerated after saturation [8].

Activation can occur by two different ways: physical or chemical activation. In the first case, it occurs a selective gasification of individual carbon atoms using carbon dioxide or water vapour at 800-900ºC, while chemical activation involves the incorporation of reagents in the precursors before carbonisation. In chemical activation, there is no selective removal of carbon atoms as during physical activation and carbonisations yields are generally improved [48, 49]. Chemical activation is therefore a simple process that increases the porosity of materials during the heat treatment. This treatment may consist of pyrolysis or microwave heating, both done under nitrogen atmosphere. In this work, the heat treatment applied was pyrolysis, therefore only this process will be emphasized. Activation could be done before pyrolysis, impregnating the precursor materials with chemical agents like KOH, NaOH, $ZnCl_2$, K_2CO_3 or H_3PO_4. Once impregnated, the materials are pyrolysed, washed with HCl to remove inorganic materials such as carbonates and ashes originated during pyrolysis, unblocking pores, and further washed with distilled water. In some cases, the washing with HCl allows the increase of the surface area up to the double of non-washed materials [40]. There is other possible way to activate the precursors that consists in pyrolyse, impregnate the materials and then pyrolyse for the second time. This two-step activation implicates greater energy spent and less mass yield but commonly allows to achieve high surface area.

Generally, the structure of activated carbons is mainly aromatic and it consists of carbon layers arranged as polynuclear aromatic molecules. In Figure 4 it is possible to observe two activated carbons produced from palm kernel shells, an agricultural residue, using K_2CO_3 (a) and $ZnCl_2$ (b) as activating agents [50]. It is possible to verify a high degree of porosity, better defined and uniform in the carbon activated with $ZnCl_2$.

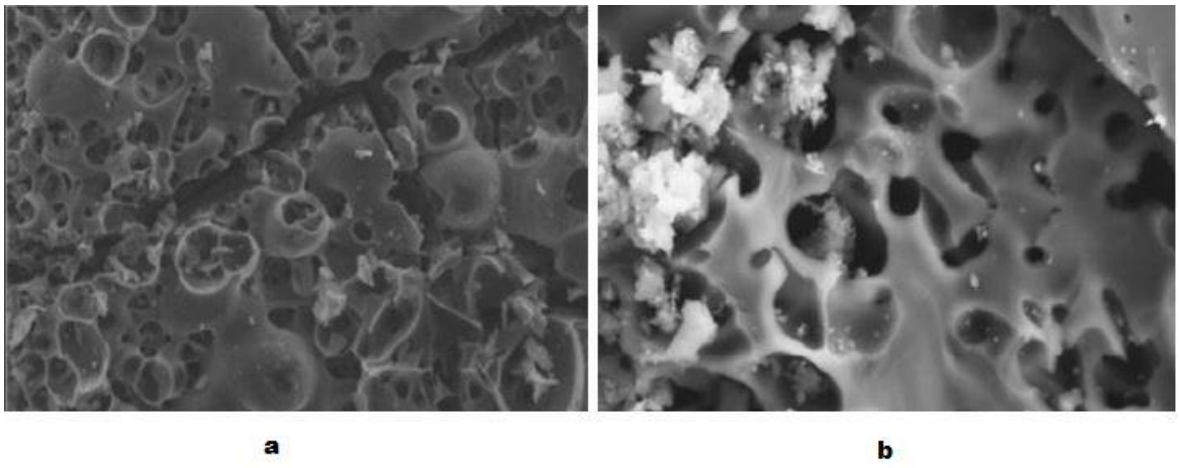

Figure 4 – SEM images of activated carbons using palm kernel shells as feedstock and K_2CO_3 (a) and $ZnCl_2$ (b) as activating agents [50]

The physical and chemical characteristics that make an activated carbon a good adsorbent are the existence of a large surface area, great porosity (with high prevalence of microporosity), high percentage of organic carbon in its composition and a low percentage of ash [41]. It is possible to predict the adsorption potential of a particular carbon based on its physicochemical properties, mainly at the surface level. In this way, multiple techniques of physicochemical characterization are usually carried out when studying the production and optimization of an adsorbent material, which are schematized in Table 2. Knowing the chemical composition of carbon surface groups, the physical structure of the carbon and the existent porosity allows us to anticipate with some assurance if the adsorption capacity of the carbon towards a specific adsorbate is high or low.

Table 2 – Physicochemical characterization techniques commonly used in the characterization of adsorbent materials

Characterization technique	Description
Proximate analysis	Chemical characterization that allows to determine moisture, volatile matter (VM), ashes and fixed carbon (FC) percentages, by the loss weight profile of the sample over a defined temperature programme and controlled atmosphere.
Total organic carbon (TOC)	TOC is obtained by the difference between total carbon (TC) and inorganic carbon (IC). Usually, the higher the TOC, the greater the potential for adsorption.
Elemental analysis	It gives the percentage of each chemical element present in the carbon, namely C, H, S, N and O.
Specific surface area	It is obtained from the BET method, which uses nitrogen isotherms to determine the extent of the carbon specific surface area (S_{BET}). Knowing that, it is also possible to calculate the total microporous volume (W_0).
Point of zero charge (PZC)	PZC provides the net charge of carbon surface. Boehm's titration gives the concentration of functional groups present on carbon surface, namely carboxylic acids, phenols, lactones and total basic groups. These two techniques complement each other. The presence of more acidic functional groups can be associated to a lower PZC, or basic groups to a higher PZC.
Boehm's titration	
Fourier transform infrared spectroscopy (FTIR)	It measures the light absorbance of the samples at wavelength in the infrared range and, by correlating these wavelengths to known standards, it is possible to identify the presence of certain functional groups in the carbon.
Scanning electron microscope (SEM)	Real images of the carbon surface are obtained, being possible to evaluate its surface roughness and texture.

2.3) Activated carbons to remove drugs from water: applications to carbamazepine and sulfamethoxazole

As previously referred, there is a wide range of pharmaceuticals found in the environment such as antibiotics, analgesics, contraceptives and others. Psychiatric drugs are amongst the most

frequently determined in aquatic environments and include sedatives, hypnotics, antidepressants, anticonvulsants, anxiolytics and antiepileptics [51]. These types of drugs have been studied in more detail only in recent years. They are the cause of an increasing public health concern due to the high rates of consumption and very specific modes of action, which leads to the difficulty of developing efficient methods to remove drugs from the environment [24].

Carbamazepine is an antiepileptic drug widely found in aqueous systems [5–7]. Its chemical structure is represented in Figure 5. It is estimated that 1014 tonnes of CBZ are consumed annually around the world [24]. The maximum concentration of CBZ found in the environment was 11.6 μg L^{-1}, a rather high value when compared with other pharmaceutical drugs [24].

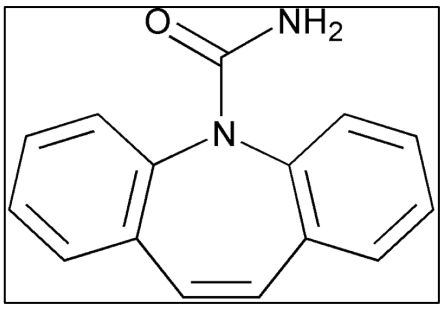

Figure 5 – Chemical structure of carbamazepine

Furthermore, as shown in Figure 6, CBZ is highly resistant to a high number of water treatment methods, with removal percentages of less than 10% for the majority of them, and the treatments with a good removal percentage, such as nano and ultrafiltration, are economical and energetically expensive.

The high frequency at which CBZ occurs in the environment and the high persistence to removal treatments and in environmental conditions makes this drug to be considered a marker of anthropogenic pollution [52, 53], being important to find a reliable and inexpensive method to remove this drug from contaminated waters. It was the case of a 2015 work that used peach stones as raw material to produce activated carbons by chemical activation with H_3PO_4 [54]. Batch and dynamic adsorption tests with this adsorbent were performed, using three different compounds: caffeine, the anti-inflammatory diclofenac and CBZ. The adsorption capacity to remove CBZ was higher than the others, reaching the maximum of 335 mg of CBZ removed for 1 g of adsorbent used [54].

Removal treatment method	% Removal	
	Diazepam	Carbamazepine
Primary treatment	< 10	< 10
COD removal (SRT* ≤ 2 days)	< 10	< 10
Nitrification (SRT 10 to 15 days)	< 10	< 10
Sludge stabilization (SRT ≥ 25 days)	< 10	< 10
Membrane bioreactor (SRT ≥ 25 days)	No data	< 10
Biofilter	No data	< 10
Soil, unsaturated zone	No data	< 10
Groundwater, saturated zone	10 - 50	< 10
Sludge anaerobic treatment	10 – 50	10 - 50
Fenton process	< 10	< 10
Effluent ozonation	10 - 50	> 90
Ozonation	10 - 50	> 90
AOPs (Advanced oxidation processes)	50 -90	50 -90
GAC (Granular activated carbon)	> 90	> 90
Ultrafiltration/PAC(Powdered activated carbon)	> 90	> 90
Nanofiltration	> 90	> 90
Chlorination	< 10	< 10
Chlordioxide	< 10	< 10

*SRT: Sludge retention time

Figure 6 – Removal percentages of two psychiatric drugs (including CBZ) from water for different treatments [24]

Sulfamethoxazole (SMX) is an antibiotic of the sulphonamide group with bacteriostatic activity. It is often administered with trimethoprim in the same formulation to treat infections such as urinary tract infections, middle ear infections, bronchitis, traveler's diarrhea, and shigellosis. Its chemical structure is shown in Figure 7.

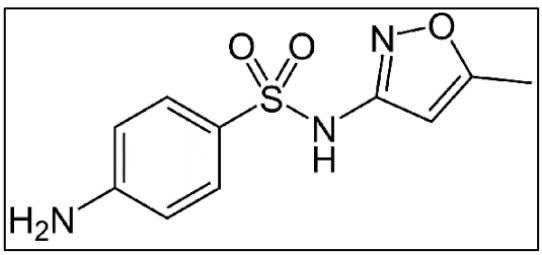

Figure 7 – Chemical structure of SMX

This antibiotic, such as the antiepileptic CBZ, is also often found in water systems [55, 56], showing the importance of developing new effective methods to remove this drug from water. As previously mentioned, the use of activated carbons as adsorbents is an interesting option. It was the case of a 2010 study that used a commercial activated carbon as adsorbent to remove two drugs from an aqueous solution: sulfamethoxazole and the anti-parasite metronidazole [57]. However, the use of the commercial carbon has made the process expensive, not following the concept of a sustainable economy. Also, Calisto et al. (2015) [13], used sludge from paper industry to produce carbons (in this case, not activated) by pyrolysis for the removal of seven different pharmaceutical compounds from water systems, where two of them were CBZ and SMX, the drugs that will be tested in this work. In Figure 8, the results of the adsorption of these pharmaceuticals using the pyrolysed carbon produced from residual sludge (PS800-150) compared to a commercial activated carbon (PBFG4) are shown. The equilibrium models of Langmuir and Freundlich were used.

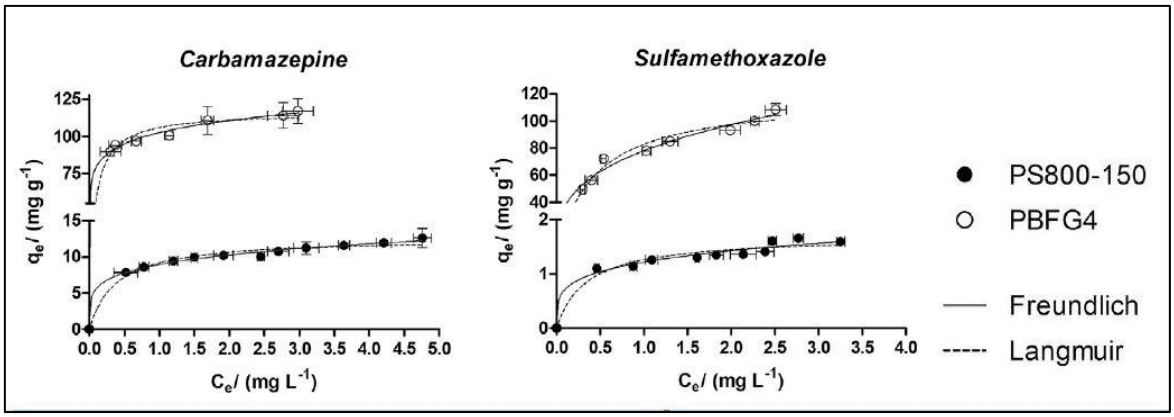

Figure 8 – Equilibrium models used to evaluate the performance of two adsorbents (PS800-150 and PBFG4) to remove CBZ and SMX from water. Adapted from Calisto et al. (2015) [13]

The adsorptive performance of the produced carbon adsorbents was low when compared with the performance of PBFG4. Therefore, it is important to investigate the production of adsorbent materials more competitive with the commercial ones.

Other works have been done, such as Yao et al. (2012) [58] who used eight different biochars to remove SMX from water. These biochars were prepared at different pyrolysis temperatures and from four different raw materials: bamboo, Brazilian pepper wood, sugarcane bagasse and hickory wood. Other authors used treated walnut shells as substrate to produce activated carbons by chemical modification [59]. In these two works, it was possible to successfully remove SMX from the contaminated aqueous solutions. None of these two works presented a comparison with commercial

adsorbents, not being possible to conclude if the produced materials are competitive with the already existing materials or not.

However, few works with activated carbons to remove CBZ and SMX from aqueous solutions can be found in literature, which makes important to research and apply alternative methods to produce activated carbons from low-cost materials, capable to remove these compounds by adsorption.

3) Obtainment of value-added products from alternative precursors

Sludge from the pulp and paper production process, as mentioned before, have potential to be used as raw material to produce adsorbents with good efficiency. However, there are other products derived from the same industry, raw (RP) and bleached pulp (BP), with similar characteristics to sludge. Given the similar composition, RP and BP may also have good potential to be used as precursors to generate adsorbents, presenting some advantages comparing to sludge: their composition is more stable and have less inorganic content, which expectedly allow to produce carbons with a higher organic carbon percentage than carbons obtained from sludge.

The use of pulps from the paper production process as raw materials for activated carbons production fits within the concept of sustainable economy, since value-added products with interesting applications are obtained from alternative precursors, and it's a new concept because it has never been tried.

4) Main goals

This work aims to:

1) Produce non-activated and activated carbons from BP and RP, in order to assess the suitability of these raw materials;
2) Characterize physically and chemically the produced carbons through different techniques;
3) Evaluate the adsorptive performance of the carbon adsorbents in ultra-pure water and WWTP effluents to remove CBZ and SMX from the water;
4) Conclude which pulp (raw or bleached) and which conditions concerning the production process are the most adequate for the production of a high performance activated carbon.

II. Materials and Methods

1) Production of carbon adsorbents

The precursors used in this work were RP and BP, provided by a local paper mill industry. This industry uses a kraft elemental chlorine free pulp production process and operates using *Eucalyptus globulus* wood. Its production reaches about 320000 tons of BP per year [60]. The pulp manufacturing process comprises three main steps until the final product: cooking, washing and bleaching. After the washing step, washed RP is obtained; subsequently, in the bleaching process, the RP obtained earlier increases its degree of whiteness by removing or modifying chromophore groups present in the pulp structure, through application of carbon dioxide and alkaline extraction stages. Similarly, after bleaching, the pulp is washed to obtain washed BP. From these two pulps, twelve different carbons were produced: six from RP and six from BP. The RP and BP provided by the paper mill are shown in Figure 9.

Figure 9 – Raw (left) and bleached (right) pulp used as carbon adsorbents precursors

Within the six carbons produced from each precursor, two were only pyrolysed, two other were pyrolysed and then acid washed with HCl 1.2 M and two were activated with two different activating agents (K_2CO_3 and H_3PO_4), pyrolysed and acid washed. In Table 3, it is possible to see all the production processes, the temperatures used in pyrolysis (500 ºC and 800 ºC), the resulting carbons and their designation. The pulp fibres were impregnated with the activating agent in a ratio of 1:1 (*w/w*). For the carbons activated with K_2CO_3, the activating agent was dissolved in distilled water with a proportion of 3:10 (*w/v*). For H_3PO_4 activation, the activating agent was diluted in a ratio of 1:8 (*v/v*). In both cases, the pulp was impregnated for 1 hour with the activating agent solution, using an ultrasonic bath at room temperature. The resulting mixture was spread on a tray and allowed to dry, at room temperature, in the fume hood for about one week. The dried pulps were then placed in porcelain crucibles for pyrolysis which was carried out under a nitrogen flow at 500 and 800 ºC with a heating rate of 10 ºC min^{-1} and with 150 minutes of residence time.

Table 3 – Adsorbents production process and carbon's designation

Carbon designation	Production step			
	Precursor	Impregnation (activating agent)	Pyrolysis (temperature)	Acid washing with HCl 1.2 M and distilled water
RP500	Raw pulp	X	500ºC	X
BP500	Bleached pulp	X	500ºC	X
RP500-HCl	Raw pulp	X	500ºC	√
BP500-HCl	Bleached pulp	X	500ºC	√
RP800	Raw pulp	X	800ºC	X
BP800	Bleached pulp	X	800ºC	X
RP800-HCl	Raw pulp	X	800ºC	√
BP800-HCl	Bleached pulp	X	800ºC	√
RP800-HCl-K_2CO_3	Raw pulp	K_2CO_3	800ºC	√
BP800-HCl-K_2CO_3	Bleached pulp	K_2CO_3	800ºC	√
RP800-HCl-H_3PO_4	Raw pulp	H_3PO_4	800ºC	√
BP800-HCl-H_3PO_4	Bleached pulp	H_3PO_4	800ºC	√

After pyrolysis, the activated carbons and two non-activated carbons from each pulp were acid washed with HCl 1.2 M by placing carbons and acid in the same container for 1 hour. It was used a proportion of 1 L of HCl 1.2 M to 30 mg of carbon adsorbent. Then, the suspension was filtered in a vacuum system and washed with distilled water until reaching neutral pH. After that, all carbons were dried in an oven at 105 ºC for 24 hours and crushed mechanically. The weights of the carbon adsorbents were measured before and after pyrolysis and after the acid washing to determine the yields of production.

2) Physical and chemical characterization of raw materials and carbon adsorbents

2.1) Total organic carbon

TOC was determined for both precursors and for all carbon adsorbents by the difference between total carbon content and inorganic carbon content, which were obtained through a TOC analyser (TOC-VCPH Shimadzu, solid sample module SSM-5000A). Glucose ($C_6H_{12}O_6$, 40% of carbon) were used as standard to obtain the calibration curve for TC determination, while sodium carbonate (Na_2CO_3, 11% of carbon) were used as the standard for IC determination. Carbon content was determined as the average of three replicates, using 30 mg of sample on each replicate.

2.2) Thermogravimetric and proximate analysis

The thermogravimetric analysis (TGA) and proximate analyses were made for the precursors and for the produced carbon adsorbents and were carried out in a thermogravimetric balance Setsys Evolution 1750, Setaram, TGA mode (S type sensor). Standard methods to determine the moisture (UNE 32002) [61], volatile matter (UNE 32019) [62] and ash content (UNE 32004) [63] were employed. The fixed carbon was determined as the remaining fraction after ash and volatile matter (at dry basis) determination. The experimental procedure for TGA consisted of the sample heating, under nitrogen atmosphere, from the room temperature to 105 ºC (heating rate of 10 ºC min^{-1}); sample was kept at this temperature until total stabilization of the weight (approximately 30 min); next, temperature was increased from 105 to 950 ºC (10 ºC min^{-1}), keeping the sample at 950 ºC until total stabilization of the weight (approximately 30 min); finally, at 950 ºC, the carrier gas was automatically switched to air and the sample was maintained at 950 ºC until total stabilization of the weight. The mass loss observed around 105 ºC is attributed to moisture; the mass loss registered from the end of this first step up to the switching of the carrier gas corresponds to volatile matter; the mass loss comprised between the introduction of the air flow and the stabilization of the weight is attributed to fixed carbon content; and lastly the final residue corresponds to ash content.

2.3) Elemental analysis

Elemental analysis was determined for the precursors and for all carbon adsorbents. The acquisition of the data of elemental analysis involving the determination of the sample content in C, H, N and S was performed in a LECO TruSpec CHNS Micro analyser, using sulfamethazine as calibration standard. The percentage of oxygen was calculated, at a dry basis and after correction of ash content, by difference between 100% and the total percentages of C, H, N and S.

2.4) Fourier transform infrared spectroscopy with attenuated total reflectance

The Fourier transform infrared spectroscopy with attenuated total reflectance (FTIR-ATR) spectra were acquired through a Shimadzu-IRaffinity-1, using an attenuated total reflectance (ATR) module, with a nitrogen purge. The measurements were recorded in the range of 600-4000 cm^{-1} wavenumbers, 4.0 of resolution, 128 scans and with atmosphere and background correction. Both precursors and all produced carbons were measured.

2.5) Point of zero charge

The point of zero charge (PZC) of the carbons was determined only for carbon adsorbents by the pH variation of a solution with a known pH after contact with each of the carbon (pH drift method [64]). Ten solutions of NaCl 0.1M with pH ranging between 2 and 11 were prepared by adjusting the pH with HCl 0.1 and 0.05 M and NaOH 0.05 and 0.1 M. After that, 10 mL of each solution were transferred to a polypropylene tube containing 2 mg of carbon. All carbons were shaken with the solutions of different initial pH (pH_i) at 40 rpm overnight at 25 ºC in an overhead shaker (Heidolph, Reax 2). Later, the final pH (pH_f) was measured. Then, the PZC was determined by plotting ΔpH ($pH_f - pH_i$) versus pH_i and the PZC corresponds to the pH value where the curve crosses the x-axis [41].

2.6) Boehm´s Titration

The quantification of functional groups present on carbons surface was determined only for the produced carbons by the Boehm's method [65]. Accordingly, each carbon was added to NaOH 0.05 M, $NaHCO_3$ 0.05 M, Na_2CO_3 0.05 M or HCl 0.05 M solutions into polypropylene tubes at a final concentration of 10 g L^{-1}, under nitrogen atmosphere. The mixtures were then shaken inside a thermostatic incubator at 25 °C for 24 h. After, the supernatants were filtered and 25 mL of each one were titrated with 0.1 M HCl or 0.1 M NaOH solutions in order to quantify the total acid and basic functional groups, respectively. In addition, the different acidic groups on the carbons surface were determined as follows: the amount of carboxyl groups was estimated by neutralization with $NaHCO_3$ solution; the amount of lactones was obtained from the difference between the neutralization with Na_2CO_3 solution and that determined for the $NaHCO_3$ solution; and the amount of phenols was estimated from the difference between the neutralization with NaOH solution and that determined for the Na_2CO_3 solution. Furthermore, NaOH and HCl solutions were standardized with $C_8H_5KO_4$ and Na_2CO_3 solutions, respectively, for the determination of their exact concentration.

2.7) Specific surface area and porosity

Specific surface area (S_{BET}) and total micropore volume (W_0) were determined only for carbon adsorbents by nitrogen adsorption isotherms. These isotherms were acquired at 77 K using a Micromeritics Instrument, Gemini VII 2380 after outgassing the materials overnight at 120 ºC. S_{BET} was calculated from the Brunauer-Emmett-Teller equation [16] in the relative pressure range 0.01-0.1. Total pore volume (V_p) was estimated from the amount of nitrogen adsorbed at a relative pressure of 0.99. W_0 was determined by applying the Dubinin-Radushkevich equation [66] to the lower relative pressure zone of the nitrogen adsorption isotherm.

2.8) Scanning electron microscopy

Scanning electron microscopy (SEM) images were obtained at different magnitudes using a Hitachi SU-70 in order to observe the superficial morphology of the precursors and the produced carbon adsorbents. The magnitudes applied were 300x, 1000x, 3000x, 10000x, 30000x and 50000x.

3) Batch adsorption experiments

In order to test the adsorptive performance of the produced carbons for the removal of pharmaceuticals from water, adsorption tests were made in batch conditions: kinetic and adsorption equilibrium experiments. Two different drugs were used in these tests: the antiepileptic CBZ and the antibiotic SMX. In all tests, the initial drug concentration was 5 mg L^{-1}. Two different matrices were used: the performance of the carbons was firstly evaluated in ultra-pure water and then in the final effluent (after secondary treatment, as discharged into the environment) of a WWTP. This effluent was collected from the urban WWTP of *Costa de Lavos* (Figueira da Foz), Portugal (Figure 10). Effluent was sampled at two different times – firstly to perform adsorption tests with CBZ (effluent 1) and lastly to perform the same tests with SMX (effluent 2).

Figure 10 – Collection of effluents on wastewater treatment plant of *Costa de Lavos* (Figueira da Foz), Portugal

The effluent was filtered with cellulose Supor-450 Membrane Disc Filters 0.45 µm, immediately after collection, with a vacuum system to remove suspended organic matter. After filtration, the samples were stored in the dark at 4 ºC until use, for a maximum period of 10 days. The pH, conductivity and dissolved organic carbon (DOC) of the filtered effluent were measured.

For all the adsorption experiments, carbon adsorbents were weighted on a microbalance with an uncertainty of ± 0.001 mg. A known mass of carbon adsorbent was shaken with the drug solution at 80 rpm in an overhead shaker (Heidolph, Reax 2) at 25 ºC, using polypropylene tubes**.** Experiments were run in triplicate. After shaking, the solution of each tube was filtered through Whatman PVDF Membrane Filters 0.22 µm to remove the tested carbon adsorbent from solution and stop the adsorption process. After that, the solution was analysed by capillary electrophoresis, in order to determine the remaining drug concentration, in accordance with the procedure described in section **II-3.5**. In all experiments, the pharmaceutical solution was also shaken without the presence of the adsorbent as control testing.

3.1) Adsorption preliminary tests

Before carrying out kinetic and adsorption equilibrium experiments, preliminary tests were performed with all carbon adsorbents with the purpose of concluding about the materials that have the best adsorptive removals and then choose the two best adsorbents to study their kinetical behaviour and define their isotherms in equilibrium conditions. For that, different adsorbent's concentrations were tested for all materials with overnight shaking at 80 rpm, ensuring enough time to reach the adsorption equilibrium. The adsorbent's concentrations used in the preliminary tests can be consulted in Table 4.

Table 4 – Adsorbent's concentration used in preliminary tests for the removal of CBZ and SMX (at an initial concentration of 5 mg L^{-1})

<table>
<tr><td rowspan="3">Carbon adsorbents</td><td colspan="3">CBZ 5 mg L^{-1}</td><td colspan="2">SMX 5 mg L^{-1}</td></tr>
<tr><td rowspan="2">Ultra-pure water</td><td colspan="2">WWTP effluent</td><td rowspan="2">Ultra-pure water</td><td rowspan="2">WWTP effluent (Effluent 2)</td></tr>
<tr><td>Effluent 1</td><td>Effluent 2</td></tr>
<tr><td></td><td colspan="4">Carbons mass concentrations (g L^{-1})</td></tr>
<tr><td>Non-activated carbons</td><td>0.15; 0.50</td><td colspan="2">-</td><td>-</td><td>-</td></tr>
<tr><td>RP800-HCl-K_2CO_3</td><td rowspan="4">0.05; 0.15</td><td colspan="2">-</td><td rowspan="4">0.05; 0.10</td><td>-</td></tr>
<tr><td>BP800-HCl-K_2CO_3</td><td colspan="2">-</td><td>-</td></tr>
<tr><td>RP800-HCl-H_3PO_4</td><td>0.035; 0.05; 0.07</td><td>-</td><td rowspan="2">0.07; 0.10</td></tr>
<tr><td>BP800-HCl-H_3PO_4</td><td>0.07</td></tr>
</table>

The amount of the target pharmaceutical adsorbed onto the corresponding adsorbent, q (mg g^{-1}), was calculated by Equation 1.

3.2) Kinetic adsorption studies

Kinetic adsorption studies were made only for the two best adsorptive performance carbons, selected in adsorption preliminary tests. These studies followed the procedure explained above with the difference that a fixed mass concentration of each carbon adsorbent was employed and the varying factor was the shaking time of the carbon adsorbents with the drug solutions. In all kinetic experiments shaking times of 5, 15 and 30 minutes, 1, 2 and 4 hours were used. In tests with real effluents, were also used additional shaking times of 8, 10, 14 and 18 hours. For tests with CBZ, the mass concentrations used were 0.035 and 0.070 g L^{-1} in ultra-pure water and WWTP effluents, respectively, and for tests with SMX were 0.035 and 0.3 g L^{-1} in the same matrices. The amount of the target pharmaceutical adsorbed onto the corresponding adsorbent, q_t (mg g^{-1}), for each shaking time, was calculated by Equation 1, and the experimental data were fitted to a pseudo-first and pseudo-second order kinetic models (Equations 6 and 7, respectively) in order to determine the kinetic parameters of the experiments, namely the amount of pharmaceutical adsorbed when the equilibrium is attained, q_e (mg g^{-1}), the pseudo-first order rate constant, k_1 (min^{-1}), and pseudo-second order rate constant, k_2 (g mg^{-1} min^{-1}).Three fit parameters (R^2, ASS and $S_{y/x}$) were determined to evaluate the goodness of fit. GraphPad Prism 5 software was used for the nonlinear regression fittings.

3.3) Equilibrium adsorption studies

Equilibrium adsorption studies were made also only for the two best adsorptive performance carbons, selected in adsorption preliminary tests. These experiments were performed using as shaking time the one determined in the kinetic studies of each system (t_S). All tests were carried out at 80 rpm under 25 ºC, varying the carbon absorbents concentrations, as described in Table 5.

The amount of the target pharmaceutical adsorbed onto the corresponding adsorbent q_e (mg g^{-1}), was calculated by Equation 1 and the experimental data were fitted to the Langmuir, Freundlich and Langmuir-Freundlich equilibrium models (Equations 2,4 and 5, respectively) in order to determine the equilibrium parameters of the systems. Three fit parameters (R^2, ASS and $S_{y/x}$) were determined to evaluate the goodness of fit. GraphPad Prism 5 software was used for the nonlinear regression fittings.

Table 5 - Adsorbent's concentration and shaking time used on adsorption equilibrium experiments for CBZ and SMX 5 mg L^{-1}

Carbon adsorbents	**CBZ 5 mg L^{-1}**				**SMX 5 mg L^{-1}**			
	Ultra-pure water		WWTP effluent		Ultra-pure water		WWTP effluent	
	Conc. (g L^{-1})	ts (h)	Conc. (g L^{-1})	ts (h)	Conc. (g L^{-1})	ts (h)	Conc. (g L^{-1})	ts (h)
RP800-HCl-H_3PO_4	0.11; 0.080; 0.070; 0.060; 0.050; 0.040; 0.035; 0.030	3	0.30; 0.25; 0.20; 0.15; 0.13; 0.11; 0.090; 0.070; 0.050; 0.040	15	0.090; 0.080; 0.070; 0.060; 0.050; 0.040; 0.035; 0.030	4	0.70; 0.60; 0.50; 0.45; 0.40; 0.35; 0.30	19
BP800-HCl-H_3PO_4	0.090; 0.080; 0.070; 0.060; 0.050; 0.040; 0.035; 0.030		0.15; 0.10; 0.080; 0.070; 0.060; 0.050; 0.040; 0.030; 0.025; 0.020	15	0.080; 0.070; 0.060; 0.050; 0.040; 0.035; 0.030; 0.025		0.70; 0.60; 0.50; 0.40; 0.30; 0.20; 0.15; 0.10; 0.090	16

3.4) Kinetic and isotherm models - fitting parameters

Three main parameters were determined to evaluate the quality of the fitting of the selected models to describe kinetic and equilibrium experiments data. All of them were given by the software GraphPad Prism 5. They are:

- Correlation coefficient, R^2

$$R^2 = 1 - \frac{SS_{regression}}{SS_{total}}$$

Equation 8

where $SS_{regression}$ is the sum of squares of the regression and SS_{total} is the total sum of squares;

- Absolute sum-of-squares (ASS)

The absolute sum-of-squares of the nonlinear regression ($\sum[y_i - \hat{y}]^2$) is the distance value of the data points (y_i) from the regression curve ($\hat{y}$);

- Standard deviation of residuals, $S_{y/x}$

$$S_{y/x} = \sqrt{\frac{\sum(residual^2)}{n - K}}$$

Equation 9

where *K* is the number of parameters fitted by the regression and *n* is the number of points of the regression. The residual is the vertical distance (in Y units) of the experimental point to the fitted curve.

3.5) Quantification of drugs by capillary electrophoresis

The quantification of CBZ and SMX concentrations was performed by capillary electrophoresis, using a Beckman P/ACE MDQ (Fullerton, CA, USA) instrument, equipped with a UV/VIS detector and controlled by the software 32 Karat. The separation was made using a coated fused silica capillary of 40 cm total length (30 cm to the detection window).

The used quantitative method of analysis was based in a MEKC method with capillary coating and using a sodium borate electrolyte (buffer) together with sodium dodecyl sulphate (surfactant agent). An internal standard (ethyl vanillin at final concentration of 3.4 mg L^{-1}) was added to the standards and samples before injection because the samples injection is made by pressure, and it cannot be guaranteed that the quantity of sample that enters the capillary is repeatable between injections. With the use of an internal standard, the same proportion of sample and ethyl vanillin enters at the same time allowing to correct the results from variations in the injected volume. Three replicates were always made for each one of the three replicates of the adsorption tests. All experimental conditions (Coating step, analysis parameters and separation method for drug quantification) are presented in Table 6. The experimental data were treated using Matlab 7.0 software for peaks integration.

Table 6 – Experimental conditions of the used method (MEKC) to quantify drug's concentration

Coating	20 psi: 1) NaOH 1 M (30 min) 2) H_2O (15 min) 3) Polybrene 0.5% (w/v) in NaCl 0.5 M (20 min) 4) H_2O (2 min) 5) Buffer (20 min)	
Analysis parameters	Beginning of the day	Buffer (20 min)
	End of the day	H_2O (10 min)
	Buffer	15 mM sodium borate and 30 mM SDS
	Sample preparation	1350 µL of sample + 30 µL of ethyl vanillin 167 mg L^{-1} + 150 µL of sodium borate 100 mM
	Potential supply	25 kV
	Temperature	25ºC
	Detection wavelength	200 nm
Separation method	1) Rinse the capillary with H_2O for 1 min at 20 psi 2) Rinse the capillary with buffer for 2 min at 20 psi 3) Inject sample by hydrodynamic injection for 4 s at 0.5 psi 4) Inject separation buffer for 3 s at 0.5 psi 5) Separate with separation buffer for 2.5-4 minutes	

3.6) Calibration curve

The amount of CBZ and SMX was determined using a calibration curve in the range between 0.25 and 5.0 mg L^{-1}. Seven standard solutions of each drug were prepared by dilution of a 5.0 mg L^{-1} solution: 0.25, 0.50, 1.0, 2.0, 3.0, 4.0 and 5.0 mg L^{-1}. Three replicates of each standard solution were analysed. It was obtained a linear calibration curve for each new capillary using the least-squares linear regression. The equation of the regression curve is given by:

$$y = a + bx$$

Equation 10

where y is the *ratio* between the peak area of the sample and the peak area of the internal standard, x is the concentration of solute, b is the curve slope and a is the intercept on the y-axis.

Limits of detection (LOD) and quantification (LOQ) were determined by the calibration curve method according to International Conference on Harmonization (ICH) guidelines [67]. LOD and LOQ were defined as:

$$LOD = 3.3 \times \frac{s_a}{S}$$

Equation 11

$$LOQ = 10 \times \frac{s_a}{S}$$

Equation 12

where s_a is the standard deviation of the y-intercepts and S is the slope of the calibration curve.

III. Results and Discussion

1) Thermogravimetric analysis of the precursors and production of carbon adsorbents

The thermogravimetric analysis of carbon precursors (RP and BP) was made to determine the mass loss profiles of the pulps, in order to choose the optimum temperature for the production of the pyrolysed adsorbents. The results are shown in Figure 11.

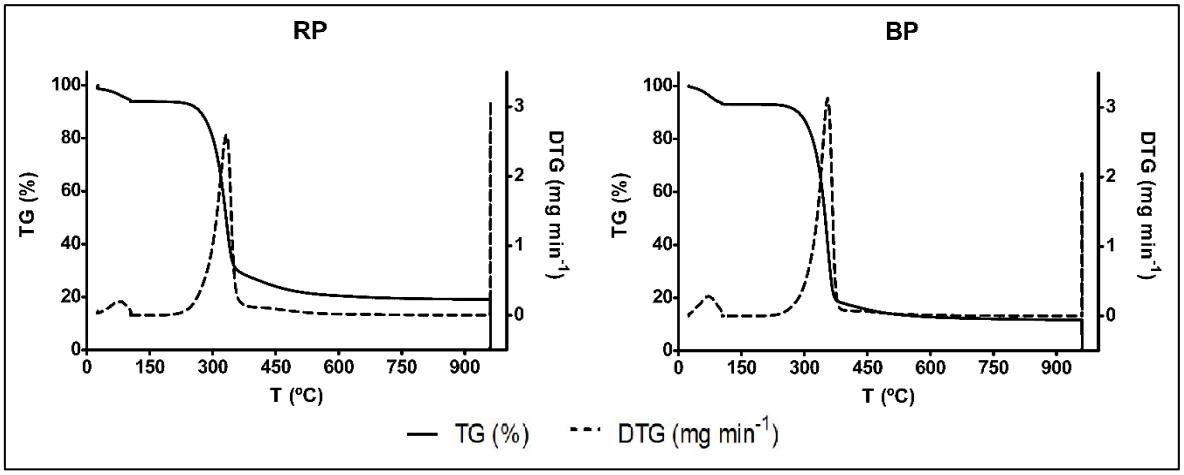

Figure 11 – Thermogravimetric (TG) and derivative thermogravimetric (DTG) analyses of raw and bleached pulps

The first derivative thermogravimetric (DTG) peak of each pulp (76 ºC for RP and 72 ºC for BP) corresponds to the mass loss derived from water evaporation. The second peaks (333 ºC for RP and 356 ºC for BP) are due to the decomposition of organic matter [45]. From these results, two different temperatures were chosen for pyrolysis: 500 ºC and 800 ºC. Both temperatures ensured the decomposition of organic. However, 800 ºC was the chosen temperature to produce activated carbons because higher temperatures usually translate into a higher development of microporosity, which is advantageous for adsorbents with superior adsorption capacity [45]. In addition, this allows for comparison among other similar works in the literature, where precursors of the same nature and equal pyrolysis temperatures (800ºC) were employed. [13, 40, 41, 45, 60].

The production yield of all carbon adsorbents was calculated in order to determine mass losses that occur during the production process. This parameter was calculated after pyrolysis and acid washing steps. The yields obtained were, on average with RP and BP-based carbons, of 21% for non-activated and non-washed carbons, 18% for non-activated and washed carbons, 19% for H_3PO_4-activated carbons and 4% for K_2CO_3-activated carbons. The differences between non-washed and washed non-activated carbons are due to the acid washing with HCl; the small decrease (from 21 % to 18 %) indicate a low content of inorganic matter of these carbons. Larger losses of material, mainly

in the carbons activated with K_2CO_3, are due to the removal of carbonates during washing. Beyond this, BP-based carbons have average yields 30% lower than RP-based carbons. This fact could be explained by the higher percentages of moisture and volatile matter present in BP, comparing with RP, as can be observed in section **III-2.2**. For the same pyrolysis temperature, it was expected to occur higher mass loss in materials with higher percentages of moisture and volatile matter.

2) Physical and chemical characterisation of raw materials and carbon adsorbents

After the production of the carbon adsorbents, eight characterization techniques were carried out, in order to better understand the physical and chemical properties of the produced materials. These tests allowed to know, in a first approach, which carbon adsorbents would have better characteristics to be applied in the removal of pharmaceuticals from water.

2.1) Total organic carbon

The TOC content of the precursors and all carbon adsorbents was determined and the results are presented in Table 7.

Table 7 – Determination of the total organic carbon (%) of all materials

Material	TC (%)	IC (%)	TOC (%)
RP	38 ± 2	0.048 ± 0.007	38 ± 2
BP	39.8 ± 0.4	0.03 ± 0.01	39.8 ± 0.4
RP500	75.9 ± 0.6	0.06 ± 0.01	75.9 ± 0.6
BP500	81.3 ± 0.4	0.07 ± 0.01	81.2 ± 0.4
RP800	82 ± 1	0.56 ± 0.02	81 ± 1
BP800	83.3 ± 0.8	0.09 ± 0.01	83.2 ± 0.8
RP500-HCl	76.8 ± 0.3	0.060 ± 0.007	76.8 ± 0.3
BP500-HCl	76.5 ± 0.5	0.080 ± 0.006	76.4 ± 0.5
RP800-HCl	82.0 ± 0.6	0.10 ± 0.02	81.9 ± 0.6
BP800-HCl	82.6 ± 0.7	0.09 ± 0.01	82.5 ± 0.7
RP800-HCl-K_2CO_3	71.4 ± 0.2	0.060 ± 0.009	71.3 ± 0.2
BP800-HCl-K_2CO_3	70.7 ± 0.6	0.12 ± 0.02	70.5 ± 0.6
RP800-HCl-H_3PO_4	58.9 ± 0.9	0.090 ± 0.003	58.8 ± 0.9
BP800-HCl-H_3PO_4	62.2 ± 0.6	0.09 ± 0.01	62.1 ± 0.6

These results highlight the minimal inorganic carbon content present in all produced materials, which is expected considering the low inorganic content of the starting materials,

constituting a great advantage of using these pulps as precursors for carbon adsorbents. The pyrolysis of the precursors caused an increase in the organic carbon of the resulting carbon materials, reaching the double in some cases. Activated carbons have less organic carbon than the others non-activated carbons; this fact could be explained by the presence of other chemical elements in the surface of the materials (namely oxygen), resulting from the activating agent used, that represent a significant part of carbon's structure.

2.2) Proximate and elemental analysis

The proximate analysis of the materials allowed to determine moisture, volatile matter, fixed carbon and ash content. Through elemental analysis, it was also possible to determine some chemical elements as carbon, hydrogen, nitrogen, sulphur and oxygen (by difference). All calculated parameters are shown in Table 8.

Table 8 – Results of proximate and elemental analysis for precursors and carbon materials

Sample	Proximate analysis (wt.%, dry basis)					Elemental analysis (wt.%, dry and ash free basis)				
	Moisture	Volatile Matter	Fixed Carbon	Ash	VM/ FC	%C	%H	%N	%S	%O *
RP	6.13	79.77	19.29	0.94	4.14	41.60	5.93	-	-	52.47
BP	6.88	87.75	11.72	0.53	7.49	42.34	5.99	0.03	-	51.63
RP500	4.83	21.54	74.92	3.54	0.29	79.42	2.44	-	-	18.15
BP500	3.11	27.91	72.09	0.00	0.39	81.30	2.28	-	-	16.41
RP800	8.37	11.38	82.96	5.66	0.14	82.70	0.96	0.05	-	16.29
BP800	6.02	8.89	90.57	0.53	0.10	83.93	0.23	-	-	15.85
RP500-HCl	4.94	19.61	79.84	0.55	0.25	77.56	2.77	-	-	19.67
BP500-HCl	4.61	19.51	79.56	0.93	0.25	78.91	2.20	-	-	18.89
RP800-HCl	8.38	7.71	91.11	1.17	0.08	85.69	0.00	0.12	-	14.19
BP800-HCl	8.04	7.50	91.78	0.72	0.08	84.88		-	-	15.12
RP800-HCl-K_2CO_3	14.92	11.72	87.84	0.44	0.13	72.79		-	-	27.21
BP800-HCl-K_2CO_3	16.36	14.64	85.36	0.00	0.17	71.82	0.94	0.05	-	27.18
RP800-HCl-H_3PO_4	17.67	23.96	55.56	20.48	0.43	68.93	1.69	-	-	29.38
BP800-HCl-H_3PO_4	14.37	27.12	56.33	16.55	0.48	73.58	4.04	-	-	22.37
* - calculated by difference at dry and ash free basis: %O=100-%C-%H-%N-%S										

From the results, it can be verified that moisture increases with material activation. The results are also consistent between proximate and elemental analysis because materials with the lowest fixed carbon content correspond to the ones with the lowest carbon and the highest oxygen

contents. It is also possible to see a decrease of volatile matter with the increase of pyrolysis temperature, meaning that the carbons produced at higher temperatures released more volatile matter and had more potential for the development of porosity (namely, microporosity), as expected. It is also possible to conclude that BP has more potential to develop a porous structure than RP because its volatile matter content is higher. These facts are proven by the results of specific surface area and total volume of pores and micropores, which are presented in chapter **III-2.5**.

The results are also in accordance with TOC analysis showing that activated carbons have other elements that represent a big part of their structure, mainly oxygen, and inorganic material (ashes) in H_3PO_4-activated carbons. The presence of a significant percentage of ashes in these activated carbons (20.48% for RP800-HCl-H_3PO_4 and 16.55% for BP800-HCl-H_3PO_4) means that activation with H_3PO_4 and pyrolysis of both RP and BP generate a big amount of ashes, which are not completely removed by the acid washing step. A high percentage of ashes in carbon's surface is generally a disadvantage for the carbons because it decreases the adsorptive performance of the materials. However, these values are still inferior to the ones obtained by Jaria et al. (2015) [41], where activated carbons produced from primary sludge had about 50% of ashes (wt.% dry basis) after activation with KOH and NaOH.

2.3) FTIR-ATR analysis

FTIR was performed to identify the main functional groups of the materials. The FTIR-ATR spectra of RP, BP and of the produced carbon adsorbents are presented in Figure 12.

The spectra of RP and BP present several typical bands of cellulose: bands at 1032, 1105 and 1160 cm^{-1} for RP and 1030, 1105 and 1161 cm^{-1} for BP, correspond to cellulosic ethers (C-O-C bonds); bands at 1053 for RP and 1051 cm^{-1} for BP cm^{-1} are attributed to C-OH stretch of primary alcohols and carbohydrates [65, 66]. All these bands disappeared in the pyrolysed materials using a temperature of 500 ºC. This is consistent with the thermogravimetric results of the precursors (section **III-1**), where the decomposition of the most thermo-labile fraction of organic matter, as cellulose, occurs between 300 and 400 ºC.

It is important to highlight the absence of the carbonates typical bands (broad band at 1415 cm^{-1} combined with a very sharp band at 870 cm^{-1} [69]) in all spectra, which confirms the low presence of inorganic carbon in all materials, as can be consulted in section **III-2.1**.

There are also two bands in BP and RP spectra that are eliminated with pyrolysis: 2898 and 3334 cm^{-1} in BP, 2982 and 3330 cm^{-1} in RP, which represent C-H stretch vibrations and –OH phenol, respectively [70].

In carbon adsorbent materials, it occurs the presence of several bands in the region between 1660 and 2000 cm^{-1}, which are related with the presence of some aromatic combination bands [69].

The bands at 1508 and 1339 cm^{-1} in RP, 1506 and 1339 cm^{-1} in BP, correspond to aromatic ring stretches [66, 68]. All bands in this region are typical of the presence of aromatic groups, which constitute the main structure of activated carbons. The presence of some bands at 3400-4000 cm^{-1} region in all produced carbons is also notable, being these bands related with OH stretching [68]. The spectra of BP800-HCl-H_3PO_4 has fewer bands in these two band zones, which might indicate some difference in the structure of this carbon adsorbent comparing with the others, which can influence the adsorptive performance of this material.

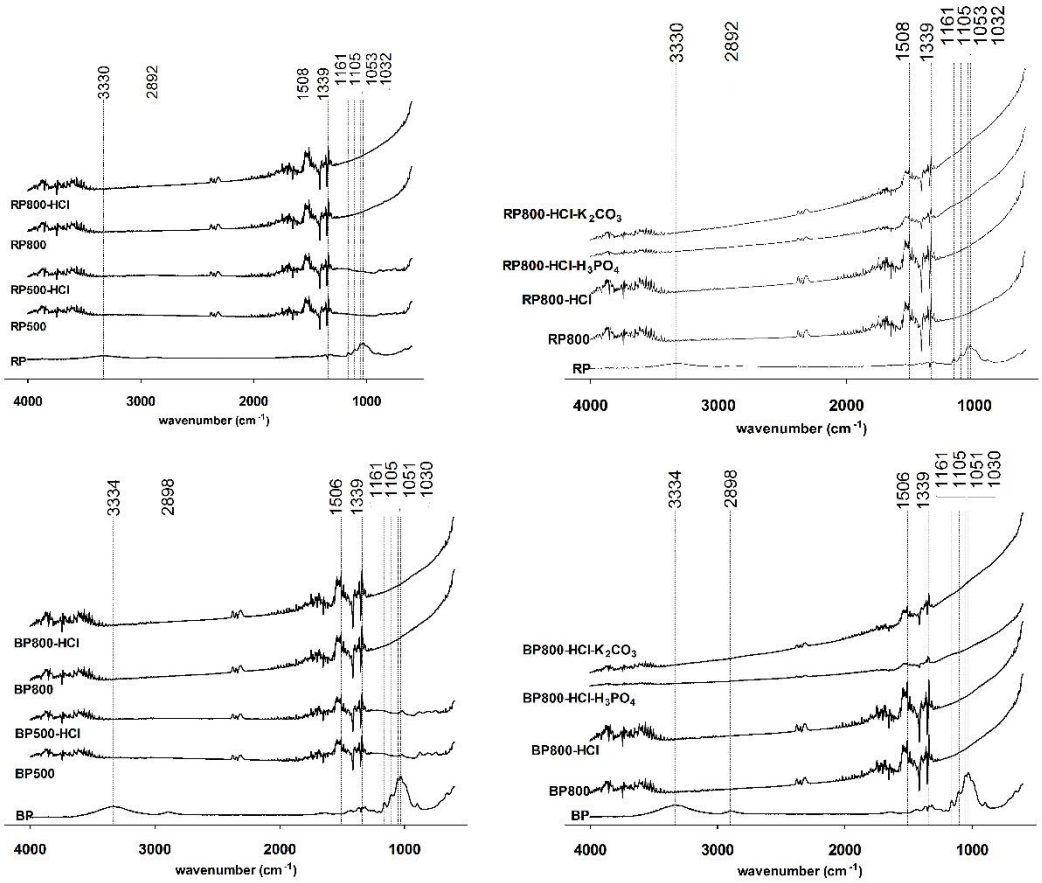

Figure 12 – FTIR-ATR spectra (absorbance versus wavenumber) of the precursors (RP and BP) and of the produced carbon adsorbents

2.4) PZC and determination of functional groups by Boehm's Titration

Being adsorption a surface phenomenon, the surface chemistry of the adsorbent materials is of utmost relevance to define interactions between adsorbents and adsorbate; thus, it is important to know which functional groups exist onto the carbons surface. For this, it was determined the PZC,

in order to know the net charge of each carbon, and the concentration of some functional groups, namely carboxyl, phenols and total basic groups. All plots for PZC determination of all produced carbons can be consulted in **Appendix 2**. In Figure 13, it is shown a graph that relates the PZC with the obtained functional groups concentrations for all produced carbon adsorbents.

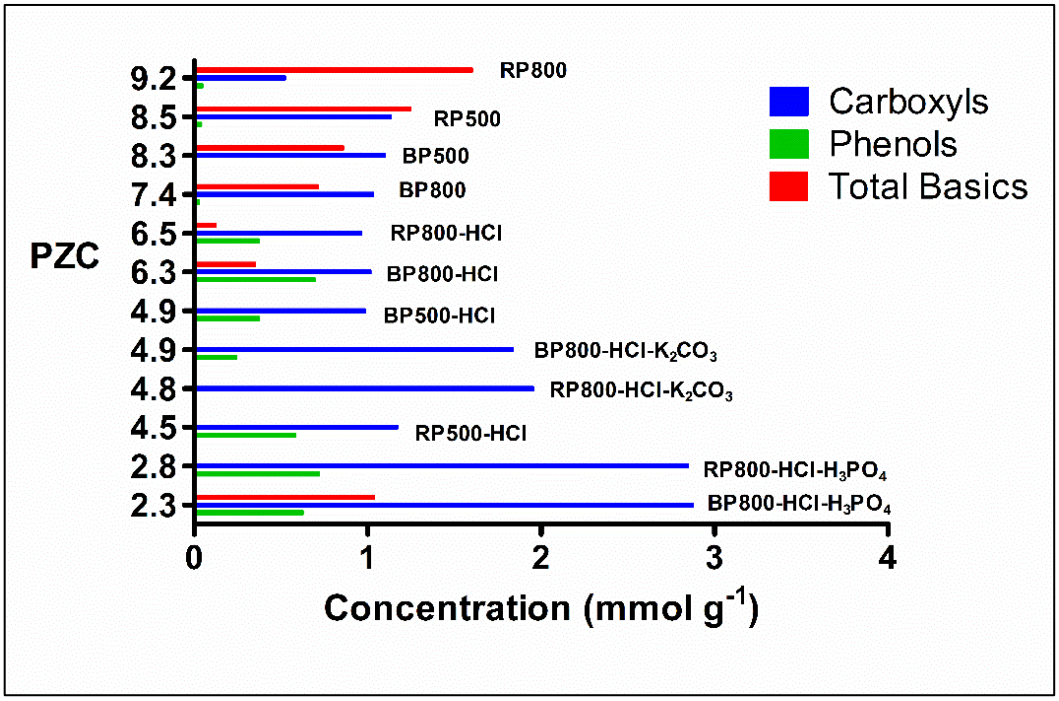

Figure 13 – Point of zero charge and functional groups concentrations of all carbon adsorbents

Since carboxyls and phenols are acidic groups, the low PZCs is directly connected with the presence of elevated concentrations of these two functional groups in the surface. On the other hand, higher PZCs are linked to a higher concentration of total basic groups and lower concentration of both carboxyl and phenol groups. These differences are important because, as it is possible to conclude later, the presence of higher concentrations of acidic groups might contribute for a better adsorptive performance of the carbon adsorbent.

In the determination of the PZC, it was also possible to verify an interesting profile of the pH of the solution, when plotting ΔpH *vs* pH_i. This effect occurred for all the carbons but was more pronounced for carbon's with neutral PZC (approximately between 6 and 7), where the lowest and highest pH of the initial solutions do not have the expected variation in contact with the carbons, being almost zero. It was the case of RP800-HCl and BP800-HCl (Figure 14), where initial solutions with pH of about 2, 3, 4, 10 and 11 did not varied after contact with the carbon adsorbent.

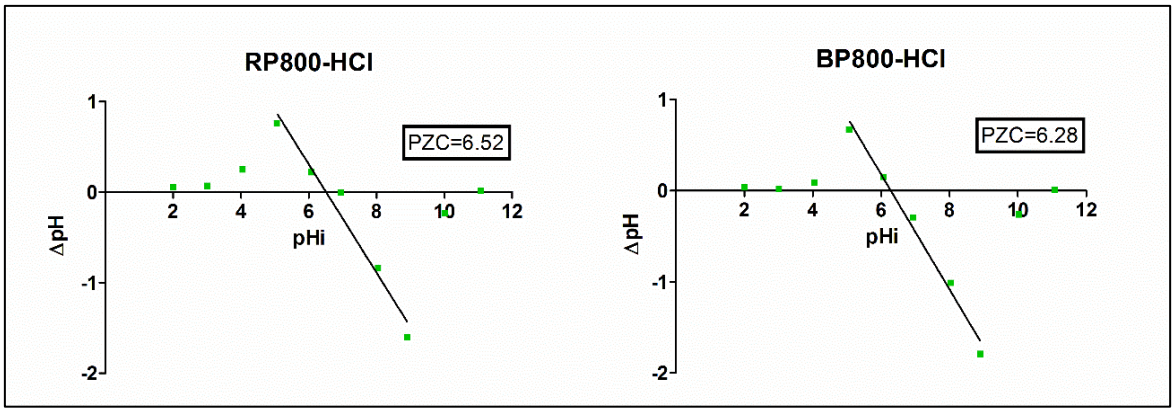

Figure 14 – Plots for PZC determination of RP800-HCl and BP800-HCl

This effect occurs because, since the carbon has a pH close to 7 on its surface, the existent functional groups are mostly weak acidic / basic groups, and are not strong enough to significantly change the pH when put in contact with solutions with very low or very high pH. Just when the initial pH of the solution approaches neutral pH, the weak functional groups that exist have a visible and measurable effect in the final pH of the solution.

2.5) Specific surface area and porosity

The physical properties of all carbon adsorbents were determined by some important parameters such as S_{BET}, V_p, W_0 and the average pore diameter (D) (Table 9).

The obtained results revealed large differences between non-activated and activated carbons, highlighting the importance of the activation step in the development of materials with higher porosity and specific surface areas. Except for those activated with K_2CO_3, all the carbons produced in the same conditions presented higher S_{BET} for BP-based carbons, compared with RP-based carbons. This fact is in accordance with the existence of more volatile matter in BP in comparison with RP, as mentioned before.

When compared with a commercially activated carbon - PBFG4 - a carbon from *Chemviron Carbon* proposed by the brand as suitable for this type of application, the results obtained for the produced activated carbons are very similar, being even better for BP800-H_3PO_4-HCl at S_{BET} and V_p parameters. The only parameter where PBFG4 is significantly better than the produced adsorbents is the total micropore volume W_0.

Table 9 – Results from the determination of the specific surface area and porosity of all produced materials and of a commercially activated carbon (PBFG4, used for comparison purposes)

Carbon adsorbent	S_{BET} (m^2g^{-1})	V_p (cm^3g^{-1})	W_0 (cm^3g^{-1})	D (nm)
RP500	3	0.002	0.000	19.00
BP500	6	0.010	0.000	7.26
RP800	3	0.003	0.001	7.90
BP800	5	0.001	0.000	9.43
RP500-HCl	6	0.004	0.001	5.95
BP500-HCl	27	0.009	0.001	5.18
RP800-HCl	27	0.003	0.001	5.17
BP800-HCl	56	0.010	0.001	5.20
RP800-HCl -K_2CO_3	855	0.065	0.018	2.69
BP800-HCl -K_2CO_3	814	0.056	0.015	2.66
RP800-HCl -H_3PO_4	768	0.311	0.137	2.33
BP800-HCl -H_3PO_4	965	0.408	0.108	2.59
PBFG4 *	848	0.360	0.295	0.84

*Parameters from Calisto et al. (2014) [45]

2.6) Scanning electron microscopy

The SEM analysis of the raw materials and produced carbon adsorbents were performed to evaluate their textural properties. The images of RP and some RP-based carbons are shown in Table 10 at a magnification of 10000x. The images of all carbon adsorbents can be seen in **Appendix 1.**

In Table 10, one can see a gradual difference between the surface morphology of the precursor (RP), where the cellulose fibres are intact, and the non-activated and non-washed carbon (RP800), where the fibres exhibit some degree of destruction with no evident porosity (as evidenced by S_{BET} analysis, presented in section **III-2.5**). The non-activated and washed carbon (RP800-HCl) did not exhibit a significant difference in comparison with RP800. However, the activated and washed carbon (RP800-HCl-K_2CO_3) has a much more modified surface with well-developed porosity and microporosity, created by the action of K_2CO_3 during activation. This fact is consistent with the results of specific surface areas and total pore and micropore volumes.

The same conclusions can be taken for the evolution from BP to some BP-based carbon (Table 11), where the activation step revealed to be, once more, the major step in the modification of the carbon external structure.

Table 10 – SEM images of RP and some RP-based carbons at 10000x

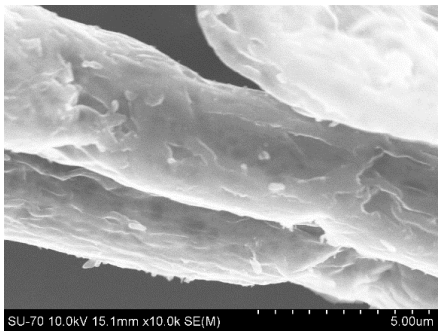 RP	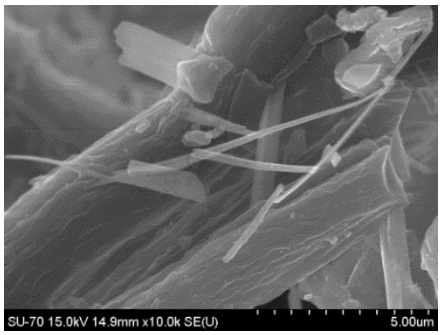 RP800
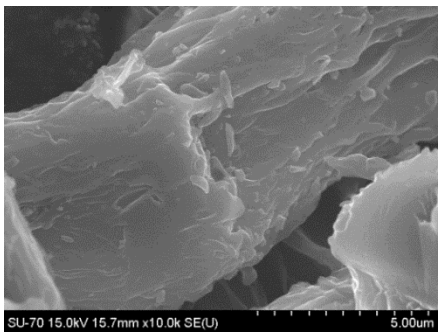 RP800-HCl	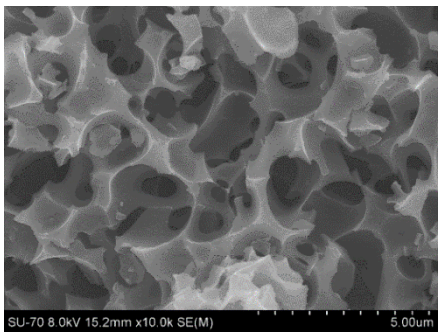 RP800-HCl-K_2CO_3

Table 11 - SEM images of BP at 3000x and some BP-based carbons at 10000x

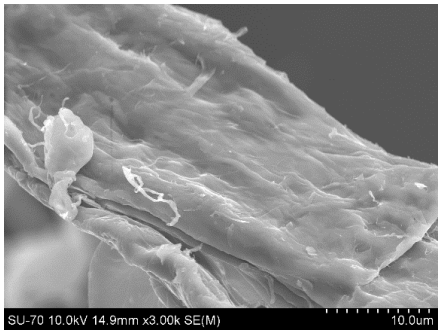 BP	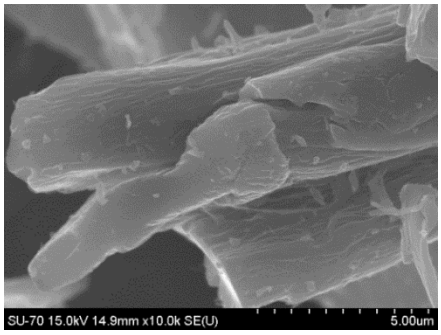 BP800
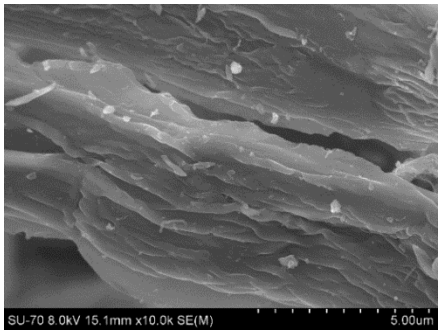 BP800-HCl	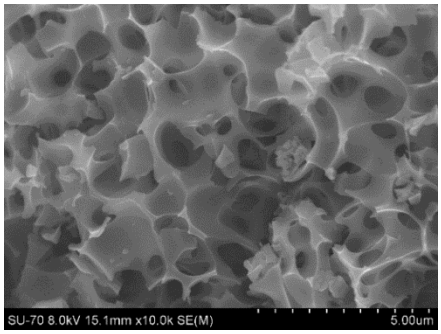 BP800-HCl-K_2CO_3

It is also important to show the differences between carbons activated with K_2CO_3 and H_3PO_4 (Table 12).

Table 12 – SEM images of all produced activated carbons at 10000x

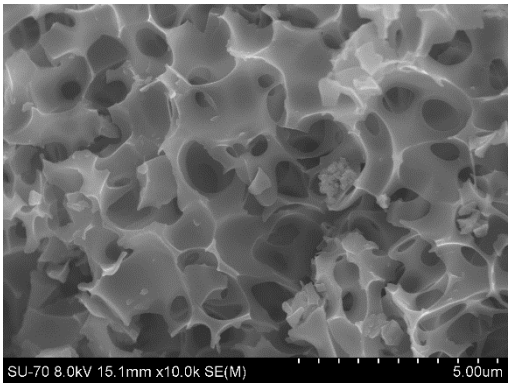 BP800-HCl-K_2CO_3	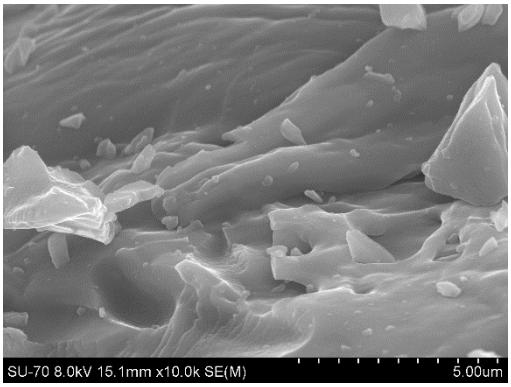 BP800-HCl-H_3PO_4
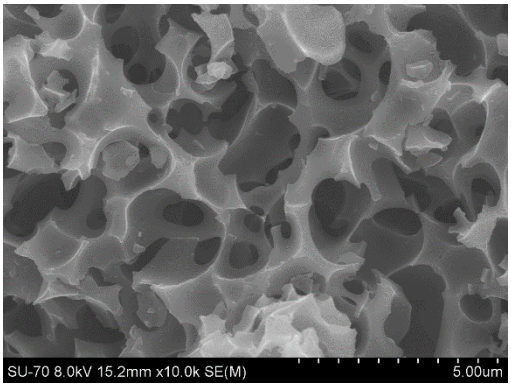 RP800-HCl-K_2CO_3	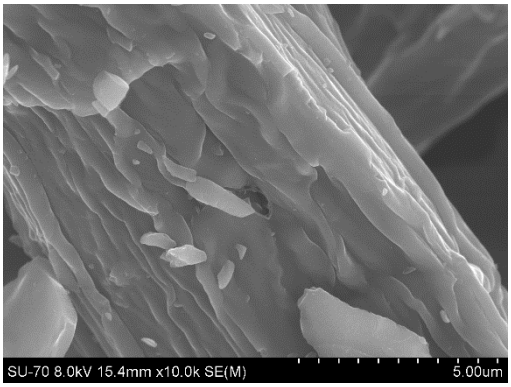 RP800-HCl-H_3PO_4

Although these images just represent the carbon adsorbents surface and do not give any information about their composition and existing functional groups, it is possible to verify a huge difference in the morphology between carbons activated with K_2CO_3 and with H_3PO_4. Carbons activated with K_2CO_3 have a rough surface with a very noticeable porosity. On the other hand, H_3PO_4-activated carbons have a smoother surface, giving the impression that the fibres of the raw materials were barely affected; it is only observable the deposition of particles onto the carbons surface which may be related to the presence of inorganic residues in the surface, as indicated by proximate analysis. This difference between the two types of activated carbons was not expected as it is not consistent with the S_{BET} analysis presented in chapter **III-2.5** seeing that both activating agents resulted in carbon adsorbents with similar S_{BET}, and the carbons with a smoother surface were the ones that reached slightly better S_{BET}. A possible explanation for the non-observed porosity in H_3PO_4-activated carbons could be the existence of a high number of micropores in these carbons, when compared with K_2CO_3-activated carbons. These micropores are not visible at the magnitudes

used in the SEM analysis, unlike the macropores and mesopores present in K_2CO_3-activated carbons, which are visible. To confirm this hypothesis, a pore distribution of all activated carbons must be done.

3) Batch adsorption experiments

3.1) Matrices

Two different matrices were used in the batch adsorption tests: ultra-pure water and urban WWTP effluents after secondary treatment. The collection of effluents was done twice: the first to perform adsorption tests with CBZ (effluent 1) and the second to perform tests with SMX (effluent 2). Two effluent collections were needed to avoid using the effluent for more than one week after collection and thus, minimize the physico-chemical alterations that can occur in the effluent, for instance, driven by microbiological action. Some characterization tests were performed to the effluents to compare them. The pH, conductivity and DOC of the effluents were measured and the obtained results are presented in Table 13.

Table 13 – pH, conductivity and DOC of the collected effluents

Sample	pH	Conductivity (ms cm^{-1})	DOC (mg L^{-1})
Effluent 1	7.31	0.26	29.3 ± 0.7
Effluent 2	7.20	1.41	9.9 ± 0.3

The results of pH were very similar between the two effluents. However, the results of conductivity and DOC were very different. Effluent 1 had approximately three times more DOC than effluent 2, which might be explained by the precipitation levels registered in the day before the collection of effluent 2, resulting in a decrease of the organic matter content in the effluents.

3.2) Calibration curve

The calibration procedure of the MEKC method was performed for each new capillary. In Figure 15, it is shown an example of a calibration curve for each drug, as well as all the parameters associated to the fitting of the linear regression.

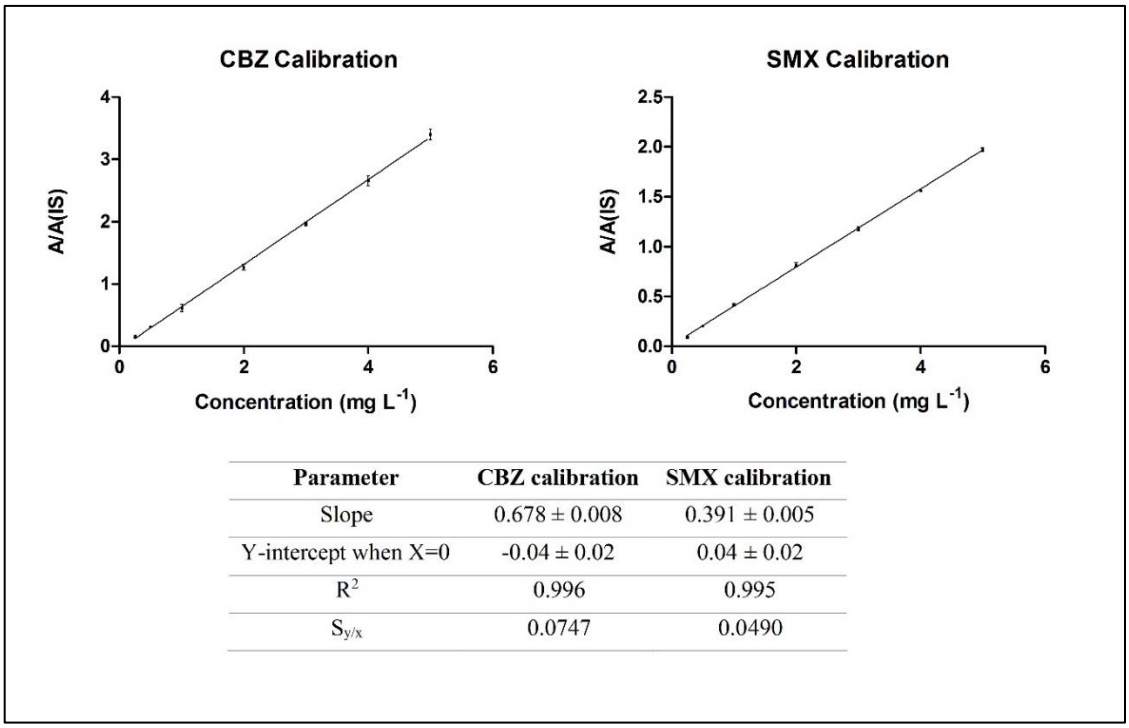

Parameter	CBZ calibration	SMX calibration
Slope	0.678 ± 0.008	0.391 ± 0.005
Y-intercept when X=0	-0.04 ± 0.02	0.04 ± 0.02
R^2	0.996	0.995
$S_{y/x}$	0.0747	0.0490

Figure 15 – Examples of a calibration curve for CBZ and for SMX and results of the parameters related to the linear regression of both curves

From these parameters, LOD and LOQ were calculated for each drug, according to the Equations 11 and 12, respectively, presented in section **II-3.6**. In these examples, the values of LOD and LOQ for CBZ were 0.11 mg L^{-1} and 0.35 mg L^{-1}, respectively, and for SMX, LOD was 0.13 mg L^{-1} and LOQ was 0.40 mg L^{-1}.

3.3) Adsorption preliminary tests

Before performing kinetic and equilibrium tests, preliminary experiments were made in order to select the best carbon adsorbents to proceed the adsorption studies. All mass concentrations of the carbons used in these experiments and the percentages of drug removed are presented in Table 14.

From the application of two different fixed masses of carbon for non-activated carbons with ultra-pure water in tests with CBZ, it was possible to conclude that these carbons did not adsorb the drug from the solution, even using higher carbon concentrations than the ones needed to achieve total removal with activated carbons; this was expected, according to S_{BET} and porosity results. As a consequence, preliminary tests with WWTP effluents were only performed with the selected activated carbons from tests with ultra-pure water because it was expected that adsorptive capacities of the carbons decrease from ultra-pure water to real effluents, and if non-activated carbons did not adsorb the drugs in ultra-pure water, they also would not be able to adsorb the drugs in real effluents. Preliminary tests with SMX in ultra-pure water using non-activated carbons were not performed

because these carbon adsorbents were unable to adsorb CBZ from the water, so the same was expected in tests with SMX.

Comparing activated carbons obtained with the considered activating agents, H_3PO_4-activated carbons systematically present better percentages of drug removal than K_2CO_3-activated carbons for CBZ and SMX, either using ultra-pure water or real effluents. For this reason, and although the use of H_3PO_4 is slightly more aggressive to the environment than K_2CO_3, it was decided to use the two carbons activated with H_3PO_4 (RP800-HCl-H_3PO_4 and BP800-HCl-H_3PO_4) to perform kinetic and equilibrium studies with the two matrices. Also, H_3PO_4-activated carbons present better production yields than K_2CO_3-activated carbons (19% and 4%, respectively). It is important to consider this factor, taking into account a possible increase in the carbons production scale.

The reason why H_3PO_4 activated carbons presented better removal percentages might be related with the total pore and micropore volumes, which are much higher than the ones obtained for K_2CO_3-activated carbons, as can be verified by the results of the specific surface areas and porosity of the materials (section **III-2.5**). However, contradictorily, these materials also have a high percentage of ashes (from approximately 17 to 20 %), which is not considered an interesting property for a carbon adsorbent. The existence of lower PZCs and a more acidic carbon surface may be other determinant factors for a better performance since H_3PO_4-activated carbons have higher concentrations of carboxyl and phenol groups in its surface structure, in comparison with K_2CO_3-activated carbons.

Table 14 – Results of preliminary tests with CBZ and SMX for all carbon adsorbents

Carbon adsorbents	CBZ 5 mg L^{-1}		SMX 5 mg L^{-1}	
	Ultra-pure water	WWTP effluent	Ultra-pure water	WWTP effluent
	Mass concentrations (g L^{-1}) | Percentage of drug removal (%)			
Non-activated carbons	0.15 | 0 0.50 | 0	-	-	-
RP800-HCl-K_2CO_3	0.05 | 54 ± 4 0.15 | 100	-	0.05 | 56 ± 2 0.10 | 92 ± 3	-
BP800-HCl-K_2CO_3	0.05 | 58 ± 7 0.15 | 100	-	0.05 | 71 ± 9 0.10 | 97.5 ± 0.4	-
RP800-HCl-H_3PO_4	0.05 | 65 ± 3 0.15 | 100	0.035 | 15 ± 5 0.05 | 24 ± 2 0.07 | 34 ± 3	0.05 | 80 ± 3 0.10 | 96 ± 2	0.07 | 0 0.10 | 0
BP800-HCl-H_3PO_4	0.05 | 85 ± 1 0.15 | 100	0.035 | 38 ± 4 0.05 | 59 ± 2 0.07 | 73 ± 3	0.05 | 82 ± 1 0.10 | 97 ± 1	0.07 | 4 ± 3 0.10 | 14 ± 3

3.4) Kinetic adsorption studies

Kinetics studies with CBZ and SMX were performed in ultra-pure water and in WWTP effluents for the two activated carbons selected in section **III-3.2**. The amount of CBZ and SMX adsorbed (q_t, mg g^{-1}) is represented versus shaking time (t) in Figure 16.

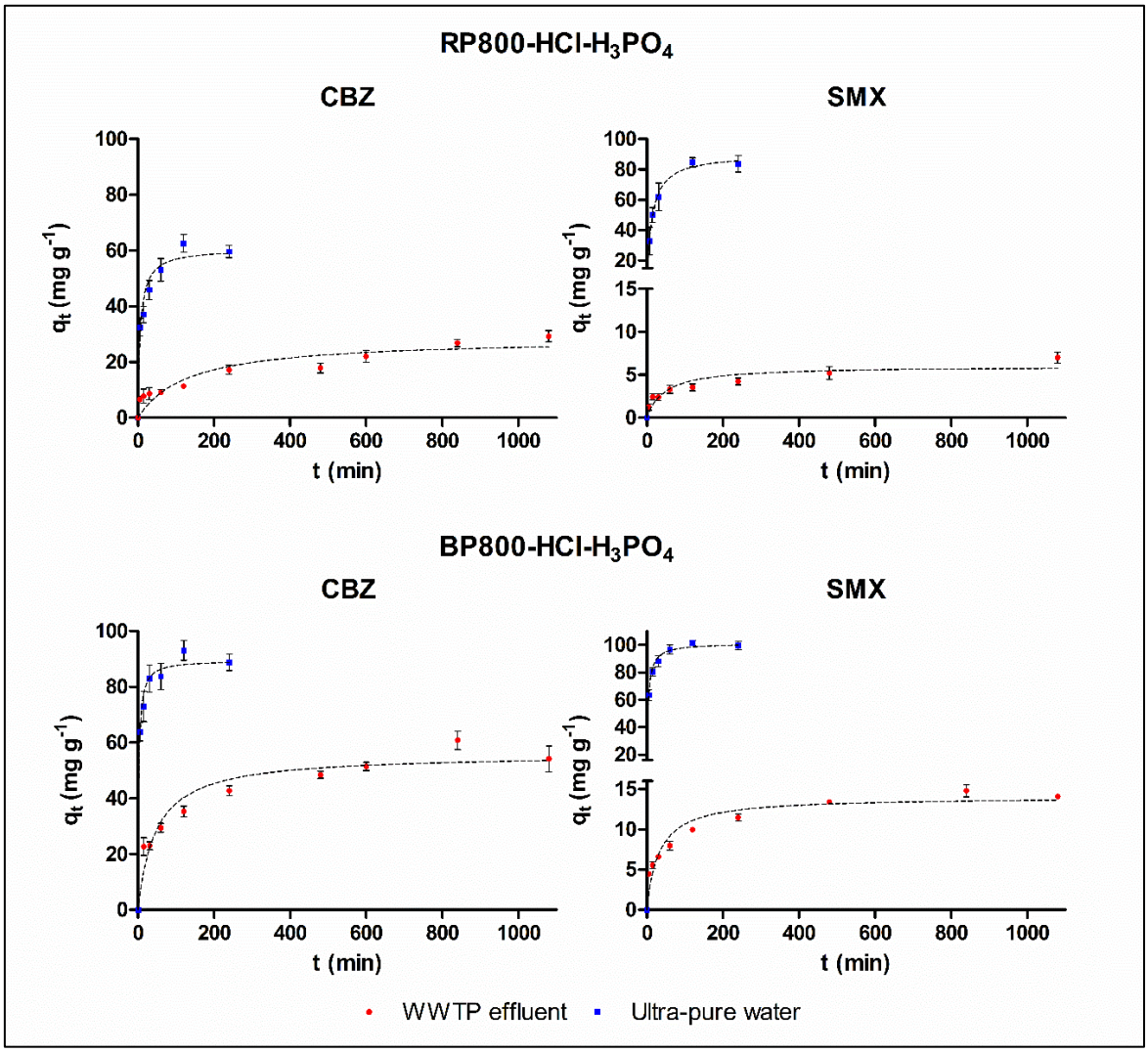

Figure 16 – Experimental data and nonlinear fit of pseudo-second order kinetic model (best fit) using, for both carbons activated with H_3PO_4, mass concentrations of 0.035 g L^{-1} in ultra-pure water for tests with CBZ and SMX; 0.070 and 0.3 g L^{-1} in WWTP effluents, for tests with CBZ and SMX, respectively

The parameters obtained from the fittings of experimental results with CBZ and SMX to the considered kinetic models (Equations 6 and 7) are summarized in Table 15 and in Table 16, respectively.

Table 15 – Fitting parameters of pseudo-first and pseudo-second order kinetic models for experiments with CBZ, using the studied adsorbents in ultra-pure water and WWTP effluents

Matrix	Adsorbent	Kinetic model	Model parameters	Fitting evaluation		
				R^2	$S_{y/x}$	ASS
Ultra-pure water	RP800-HCl-H_3PO_4	Pseudo-first order	q_e = 56 ± 4 k_1 = 0.01 ± 0.03	0.901	7.375	271.9
		Pseudo-second order	**q_e = 61 ± 3** **k_2 = 0.0030 ± 0.0009**	**0.960**	**4.712**	**111.0**
	BP800-HCl-H_3PO_4	Pseudo-first order	q_e = 85 ± 3 k_1 = 0.26 ± 0.06	0.968	6.234	194.3
		Pseudo-second order	**q_e = 90 ± 2** **k_2 = 0.005 ± 0.001**	**0.990**	**3.494**	**61.04**
WWTP effluent	RP800-HCl-H_3PO_4	Pseudo-first order	q_e = 25 ± 3 k_1 = 0.006 ± 0.002	0.813	4.165	156.1
		Pseudo-second order	**q_e = 29 ± 3** **k_2 = 0.0003 ± 0.0001**	**0.862**	**3.582**	**115.4**
	BP800-HCl-H_3PO_4	Pseudo-first order	q_e = 51 ± 3 k_1 = 0.015 ± 0.004	0.874	6.945	385.8
		Pseudo-second order	**q_e = 56 ± 3** **k_2 = 0.0004 ± 0.0001**	**0.935**	**4.979**	**198.3**
q_e (mg g^{-1}) ; k_1 (min^{-1}) ; k_2 (g mg^{-1} min^{-1})						

Table 16 - Fitting parameters of pseudo-first and pseudo-second order kinetic models for experiments with SMX, using the studied adsorbents in ultra-pure water and WWTP effluents

Matrix	Adsorbent	Kinetic model	Model parameters	Fitting evaluation		
				R^2	$S_{y/x}$	ASS
Ultra-pure water	RP800-HCl-H_3PO_4	Pseudo-first order	q_e = 83 ± 3 k_1 = 0.058 ± 0.007	0.984	4.602	84.71
		Pseudo-second order	**q_e = 90 ± 2** **k_2 = 0.00089 ± 0.00009**	**0.996**	**2.173**	**18.89**
	BP800-HCl-H_3PO_4	Pseudo-first order	q_e = 95 ± 3 k_1 = 0.19 ± 0.037	0.972	6.622	219.3
		Pseudo-second order	**q_e = 101 ± 2** **k_2 = 0.0030 ± 0.0003**	**0.996**	**2.528**	**31.95**
WWTP effluent	RP800-HCl-H_3PO_4	Pseudo-first order	q_e = 5.3 ± 0.6 k_1 = 0.017 ± 0.007	0.789	1.025	7.357
		Pseudo-second order	**q_e = 6.0 ± 0.6** **k_2 = 0.004 ± 0.002**	**0.876**	**0.785**	**4.314**
	BP800-HCl-H_3PO_4	Pseudo-first order	q_e = 13.0 ± 0.9 k_1 = 0.021 ± 0.006	0.870	1.829	26.77
		Pseudo-second order	**q_e = 14.0 ± 0.8** **k_2 = 0.0020 ± 0.0007**	**0.936**	**1.279**	**13.10**
q_e (mg g^{-1}) ; k_1 (min^{-1}) ; k_2 (g mg^{-1} min^{-1})						

Pseudo-second order was the best fitting model for all the performed tests with CBZ and SMX, according to the three fitting parameters (R^2, $S_{y/x}$ and ASS). From these results, it was possible to conclude that the adsorption was faster in ultra-pure water for most tests because k_1 and k_2 were higher in this matrix than in WWTP effluents, for the same carbon adsorbent.

By the analysis of k_2, it was possible to conclude that the difference between adsorption in ultra-pure water and WWTP effluents was more noticeable in tests with CBZ, where RP800-H_3PO_4-HCl and BP800-H_3PO_4-HCl adsorbed ten and thirteen times faster, respectively, in ultra-pure water. These results were expected due to the complex chemical composition of the secondary WWTP effluent, which contains organic and inorganic components (such as dissolved organic matter) that can compete for the adsorption sites of the carbons and, in this way, decrease the adsorption kinetics by hampering the access to the pores of the adsorbents. In tests with SMX, this kinetic difference was not so remarkable: BP800-H_3PO_4-HCl adsorbed only two times faster in ultra-pure water, and for RP800-H_3PO_4-HCl as adsorbent, the kinetic was faster in tests with WWTP effluents, through the analysis of k_2 for both matrices.

3.5) Equilibrium adsorption studies

Equilibrium adsorption tests were performed in order to evaluate the maximum adsorption capacities of the tested activated carbons. Similarly to kinetic tests, these experiments were done for CBZ and SMX, and using ultra-pure water and WWTP effluents as matrices in batch experiments. The amount of CBZ and SMX adsorbed onto ultra-pure water and WWTP effluents (q_e, mg g^{-1}) is represented *versus* the remaining concentration of drug in solution (C_e) in Figure 17. The parameters obtained from the fittings of experimental results to the considered kinetic models (Equations 2, 4 and 5) are summarized in Table 17.

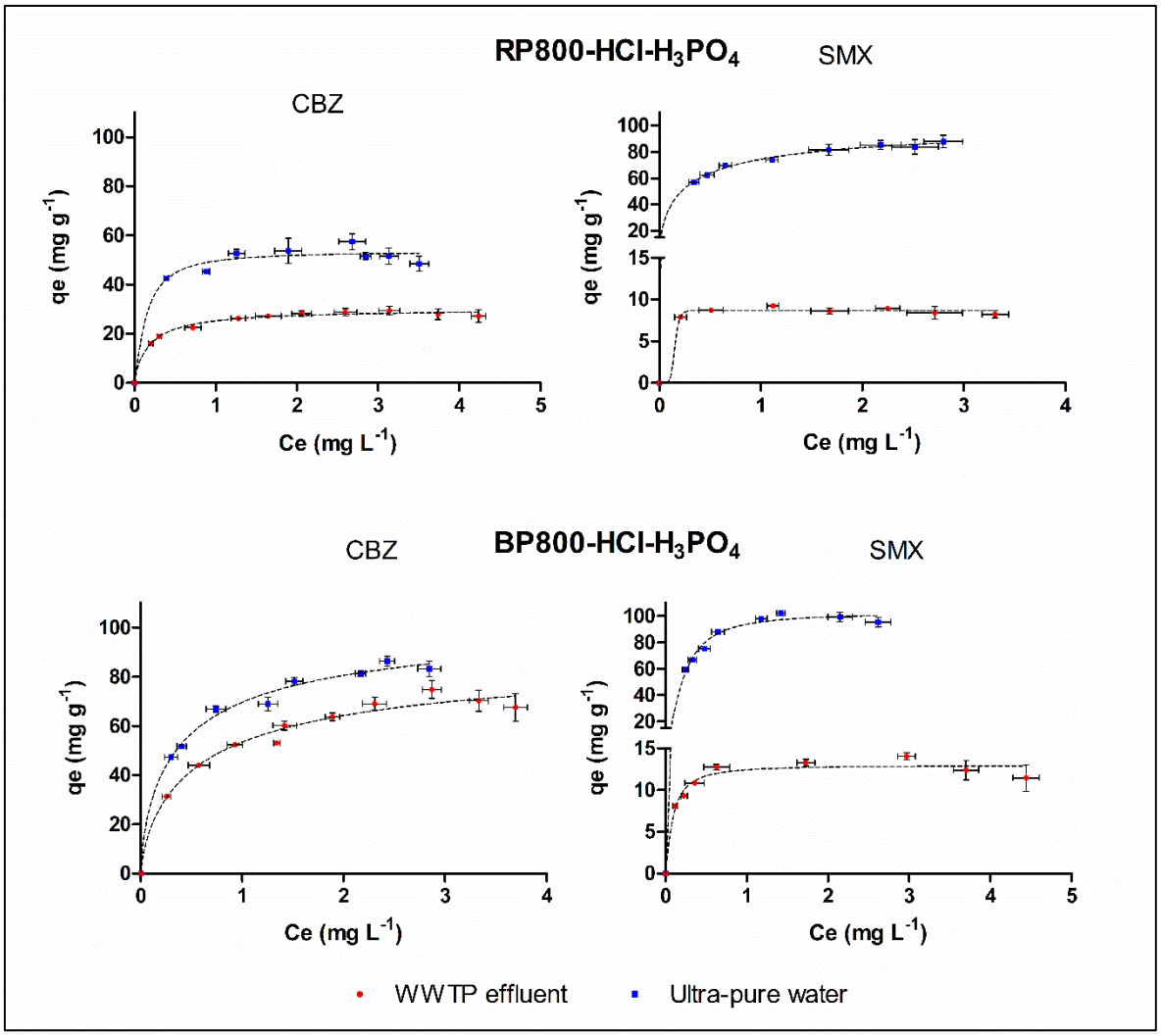

Figure 17 – Experimental data and nonlinear fit of the best-fitted equilibrium models (Langmuir-Freundlich model) for both carbons activated with H_3PO_4, for the adsorption of CBZ and SMX in WWTP effluents and ultra-pure water

Table 17 - Fitting parameters of Langmuir, Freundlich and Langmuir-Freundlich equilibrium models for experiments with CBZ and SMX, using the studied adsorbents in ultra-pure water and WWTP effluents

Adsorbate	Matrix	Adsorbent	Equilibrium model	Model parameters	Fitting evaluation		
					R^2	$S_{y/x}$	ASS
CBZ	Ultra-pure water	RP800-HCl-H_3PO_4	Langmuir	q_m = 57 ± 2; K_L = 9 ± 4	0.972	3.111	67.74
			Freundlich	K_F = 48 ± 2; n = 12 ± 5	0.965	3.479	84.72
			Langmuir-Freundlich	**q_m = 54 ± 4 K_{LF} = 12 ± 19; n_{LF} = 0.8 ± 0.8**	**0.972**	**3.336**	**66.75**
		BP800-HCl-H_3PO_4	Langmuir	q_m = 93 ± 2; K_L = 3.2 ± 0.4	0.991	2.742	52.64
			Freundlich	K_F = 67 ± 1; n = 4.0 ± 0.4	0.988	3.144	69.19
			Langmuir-Freundlich	**q_m = 107 ± 21 K_{LF} = 2 ± 1; n_{LF} = 1.4 ± 0.5**	**0.993**	**2.724**	**44.53**
	WWTP effluent	RP800-HCl-H_3PO_4	Langmuir	q_m = 29.9 ± 0.5; K_L = 5.5 ± 0.6	0.991	0.876	6.905
			Freundlich	K_F = 23.6 ± 0.6; n = 6.0 ± 0.9	0.969	1.620	23.63
			Langmuir-Freundlich	**q_m = 30 ± 1 K_{LF} = 5 ± 2; n_{LF} = 1.1 ± 0.2**	**0.991**	**0.923**	**6.820**
		BP800-HCl-H_3PO_4	Langmuir	q_m = 80 ± 3; K_L = 2.2 ± 0.4	0.978	3.420	105.3
			Freundlich	K_F = 52 ± 2; n = 3.6 ± 0.4	0.971	3.918	138.2
			Langmuir-Freundlich	**q_m = 92 ± 19 K_{LF} = 1.4 ± 0.7; n_{LF} = 1.4 ± 0.4**	**0.981**	**3.370**	**90.88**
SMX	Ultra-pure water	RP800-HCl-H_3PO_4	Langmuir	q_m = 93 ± 1; K_L= 4.5 ± 0.4	0.997	1.659	19.27
			Freundlich	K_F = 72.6 ± 0.7; n = 5.3 ± 0.3	0.996	1.828	23.40
			Langmuir-Freundlich	**q_m = 106 ± 14 K_{LF} = 2 ± 1; n_{LF} = 1.6 ± 0.5**	**0.998**	**1.461**	**12.81**
		BP800-HCl-H_3PO_4	Langmuir	q_m = 110 ± 4; K_L = 5.0 ± 0.7	0.985	4.215	124.3
			Freundlich	K_F = 88 ± 3; n = 5 ± 1	0.956	7.213	364.2
			Langmuir-Freundlich	**q_m = 102 ± 4 K_{LF} = 11 ± 6; n_{LF} = 0.7 ± 0.2**	**0.990**	**3.698**	**82.05**
	WWTP effluent	RP800-HCl-H_3PO_4	Langmuir	q_m = 8.8 ± 0.2; K_L = 55 ± 37	0.987	0.374	0.838
			Freundlich	K_F = 8.6 ± 0.2; n = 67 ± 92	0.983	0.426	1.091
			Langmuir-Freundlich	**q_m = 8.7 ± 0.2 K_{LF} = 1.38x10^{-6} ± 9x10^{-8}; n_{LF} : 0 ± 7**	**0.990**	**0.357**	**0.637**
		BP800-HCl-H_3PO_4	Langmuir	q_m = 13.3 ± 0.5; K_L = 13 ± 3	0.961	0.907	5.759
			Freundlich	K_F = 11.5 ± 0.5; n = 10 ± 4	0.918	1.317	12.13
			Langmuir-Freundlich	**q_m = 13.0 ± 0.6 K_{LF} = 22 ± 25; n_{LF} = 0.8 ± 0.4**	**0.963**	**0.950**	**5.417**

q_m (mg g^{-1}); K_L (L mg^{-1}); K_F (mg $^{1-1/n}$ L$^{1/n}$ g^{-1}); K_{LF} (mg g^{-1} (mg L^{-1})$^{-1/N_{LF}}$)

In all experiments, the best fit was always the Langmuir-Freundlich equilibrium model, according to the three fitting parameters (R^2, $S_{y/x}$ and ASS).

From the analysis of the parameters determined by the Langmuir-Freundlich equilibrium model, several conclusions can be made:

1) Except for the experiments with SMX using RP800-HCl-H_3PO_4, in ultra-pure water, the maximum adsorptive capacities were always higher for BP-activated carbon than RP-activated carbon. These results are partially justified by the higher specific surface area of BP800-HCl-H_3PO_4 (965 $m^2\ g^{-1}$), comparing with RP800-HCl-H_3PO_4 (768 $m^2\ g^{-1}$).

2) Equilibrium experiments in ultra-pure water present better or equal q_m for tests with SMX, comparing with CBZ tests in the same matrix. However, testing the drugs in WWTP effluents, q_m was significantly higher for tests with CBZ than tests with SMX. Carbon adsorbents decreased their adsorptive capacity from tests in ultra-pure water to tests in real effluents due to the presence of organic matter or other competitors in the water. However, the decrease of carbons adsorptive capacity was much higher for adsorption tests with SMX than CBZ. For tests with CBZ, the adsorptive capacities of the adsorbents decreased 45% and 14%, using RP800-HCl-H_3PO_4 and BP800-HCl-H_3PO_4, respectively, and for tests with SMX, the adsorptive capacities decreased 92% and 87% for the same carbon adsorbents.

Firstly, it was thought that this decrease in adsorption capacity could be related to the verified differences in the chemical characterization of the used effluents that were collected in two different dates (effluent 1 for CBZ and effluent 2 for SMX). To test this hypothesis, a batch test with CBZ was performed, with the same conditions of a test performed with effluent 1, but this time with effluent 2. Similar adsorption results were obtained (it was verified a negligible increase of about 0.03 % in adsorption capacity from effluent 1 to effluent 2), discarding the hypothesis of the differences in the composition of effluent 2 induced the decrease of the carbons adsorptive capacity, when tested with SMX. These results also allowed to conclude that besides the differences in conductivity and TOC between the two effluents, there was no interference of these factors in adsorption experiments of CBZ, which does not invalidate the comparison between the two drugs in real effluent.

Thus, it was hypothesised that the real reason for this accentuated decrease may lie in the carbon surface chemistry. Since the PZC of H_3PO_4-activated carbons is quite low (2.33 for BP800-HCl-H_3PO_4 and 2.83 for RP800-HCl-H_3PO_4) and the pH of WWTP effluents is close to 7, the functional groups present in the carbon surface became deprotonated, resulting in a negatively charged carbon, attracting cations and repulsing anions. Due to the pH of WWTP effluents, SMX

was negatively charged in these tests (pKa_1=1.8; pKa_2=5.7 [13]), what induced a repulsion between the drug and the groups present on the carbon surface, making difficult the adsorption process. The dissociation equilibrium of SMX for its pKa values is schematized in Figure 18.

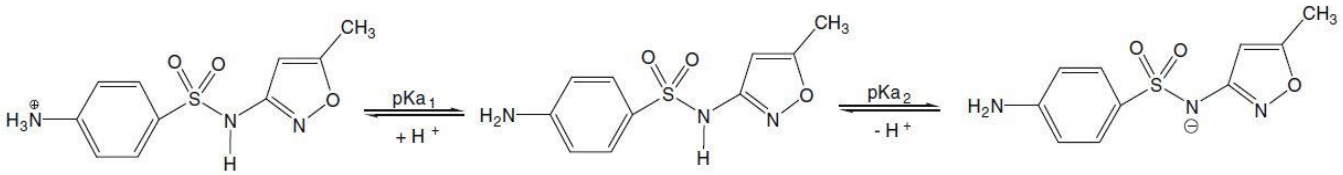

Figure 18 – Dissociation equilibrium of SMX [59]

In fact, as concluded by Teixeira et al. (2012) [59], the removal efficiency of SMX was found to be highly pH dependent. The adsorption of this drug decreased with the increase of the solution pH, as a result of increased electrostatic repulsion forces between the drug and the adsorbate.

Using ultra-pure water, which has a more acidic pH than WWTP effluents (between 5.5 and 6), there is an equilibrium between the neutral and negative species of SMX because pKa_2 of SMX is 5.7. This equilibrium decreases the electrostatic repulsion forces between the drug and the adsorbent surface, which further potentiates the adsorption in this matrix. The absence of competitors in the solution also increases the adsorption capacity of the carbon adsorbents for SMX in ultra-pure water.

The pH-dependent effect was not felt in CBZ adsorption experiments because CBZ has a neutral charge at the pH of ultra-pure water and WWTP effluents (pKa=13.9 [13]). Therefore, in this case, the observed differences between the adsorption capacities obtained between ultra-pure water and WWTP effluents are mainly due to the inhibitory effect of the competitors present in the effluents.

From all parameters determined by the Langmuir-Freundlich equilibrium model, it was possible to conclude that BP800-H_3PO_4-HCl was the carbon adsorbent with the best adsorptive performance.

3.6) Comparative study with a commercially activated carbon

The adsorptive capacity and kinetic of the best-produced adsorbent and of a commercially activated carbon (PBFG4) was compared. The physical and chemical characterization of PBFG4 were described in previous works [41, 45]. The data used in this comparative study was withdrawn from Calisto et al. (2015) [13]. All kinetic and equilibrium parameters for batch tests in ultra-pure

water with CBZ and SMX, using PBFG4 and BP800-H_3PO_4-HCl as adsorbents are summarized in Table 18.

Table 18 – Comparison of kinetic and equilibrium parameters of PBFG4 and BP800-H_3PO_4-HCl for tests with CBZ and SMX in ultra-pure water

Adsorbent		PBFG4	BP800-H_3PO_4-HCl	PBFG4	BP800-H_3PO_4-HCl
Drug		CBZ		SMX	
Kinetic studies	**Fitting parameters**	Pseudo-2nd order: q_e: 132 ± 3 k_2: 0.0011 ± 0.0002	Pseudo-2nd order: q_e: 90 ± 2 k_2: 0.005 ± 0.001	Pseudo-2nd order: q_e: 117 ± 3 k_2: 0.0021 ± 0.0004	Pseudo-2nd order: q_e: 101 ± 2 k_2: 0.0030 ± 0.0003
	R^2	0.993	0.990	0.991	0.996
	$S_{y/x}$	4.253	3.494	4.387	2.528
Equilibrium studies	**Fitting parameters**	Langmuir: q_m = 116 ± 3 K_L= 10 ± 2	Langmuir: q_m = 93 ± 2 K_L= 3.2 ± 0.4	Langmuir: q_m = 118 ± 5 K_L= 2.3 ± 0.4	Langmuir: q_m = 110 ± 4 K_L= 5.0 ± 0.7
	R^2	0.9906	0.991	0.9819	0.985
	$S_{y/x}$	3.972	2.742	4.744	4.215
q_e (mg g^{-1}); k_2 (g mg^{-1} min^{-1}); q_m (mg g^{-1}); K_L (L mg^{-1})					

The results show that the adsorption capacities obtained between the commercial activated carbon and the carbon adsorbent produced in this work are quite similar and the kinetics were faster for BP800-H_3PO_4-HCl (higher k_2), which proves the good potential of this type of precursors to produce activated carbons with good adsorptive properties. Despite the total microporous volume present in the commercially activated carbon being three times greater than the total microporous volume present in BP800-H_3PO_4-HCl (see data from chapter **III-2.5**), both adsorbents obtained similar adsorption capacities.

However, this comparative study refers to tests in ultra-pure water and do not reflect what actually happens in the environment, where wastewater has a high organic load. Although there is still no tests with PBFG4 in real effluents as matrix, the result obtained for tests with CBZ in WWTP effluents, using BP800-H_3PO_4-HCl as adsorbent (92 ± 19 mg g^{-1}) is a very promising result that indicates the good application of this carbon adsorbent in wastewater treatment.

IV. Conclusion and future prospects

Given the increase of drug's concentration in the environment, it is important to develop sustainable and effective methodologies to remove drugs from water that can compete with other existing techniques. Adsorption of drugs by activated carbons is one of these techniques and a large number of carbon adsorbents is already available in the market. The problem of the existing commercial carbon adsorbents is their high cost of production. To overcome this question and evaluate the potential of alternative precursors to produce high efficient adsorbents, the production of activated carbons from intermediate products derived from paper and pulp industry - raw and bleached pulp - was tested. Several conclusions can be made:

1) Concerning the results obtained in this work, non-activated carbons produced from the referred precursors revealed to have no potential for this application, being not able to remove CBZ from ultra-pure water. On the other hand, the activation of RP and BP with K_2CO_3 and H_3PO_4 allowed to produce four carbon adsorbents with good adsorptive performances for CBZ and SMX.

2) Activated carbons revealed interesting physical and chemical characteristics, which are correlated with a good adsorptive performance, such as an high specific surface area (S_{BET}) and a high total volume of pores and micropores, mainly for BP800-HCl-H_3PO_4 (S_{BET} of 965 m^2 g^{-1}, V_p and W_0 of 0.41 and 0.11 cm^2, respectively).

3) Evaluating the performance of activated carbons in the removal of CBZ and SMX, it was obtained a good percentage of drugs removal in ultra-pure water using a low mass concentration of carbon adsorbent (more than 90% for all four carbon adsorbents using 0.15 g L^{-1} mass carbon concentration for CBZ and 0.10 g L^{-1} for SMX). From preliminary tests using all four activated carbons in ultra-pure water and WWTP effluents, testing for CBZ and SMX, it was concluded that H_3PO_4-activated carbons were the best adsorptive performance carbons and thus, and also because of having better production yields than K_2CO_3-activated carbons, they were chosen to perform kinetic and equilibrium experiments. By studying the kinetic and equilibrium behaviour of H_3PO_4-activated carbons for both drugs and using ultra-pure water and WWTP effluents as matrices, it was possible to verify that the adsorption kinetics were slower and lower adsorption capacities were obtained for WWTP effluents with both drugs, comparing with ultra-pure water. These data should be related to the presence of competitors that influence the adsorption process and the pH effect of the solution when testing SMX.

4) From kinetic and equilibrium experiments, it was possible to conclude that the carbon adsorbent produced from bleached pulp and activated with H_3PO_4 (BP800-HCl-H_3PO_4) was the carbon

adsorbent with the best adsorptive performance. The capacity obtained for tests with CBZ and using this adsorbent as adsorbent in WWTP effluents was 92 ± 19 mg g^{-1}, being this an excellent result. When comparing BP800-HCl-H_3PO_4 with a commercial activated carbon (PBFG4) that was tested with CBZ and SMX in ultra-pure water, the produced activated carbon obtained better kinetic results and similar adsorptive capacities for the same experimental conditions. The evaluation of PBFG4 in WWTP effluents could be done, in order to compare its adsorptive performance in real effluents with the performance obtained in this work. Studies can still be carried out in order to reduce the percentage of ashes (about 17%) generated in the production of BP800-HCl-H_3PO_4, since these ashes often interfere with the carbon performance, lowering its adsorptive capacity. An economic study about the production of this carbon adsorbent could also be done.

Adsorption experiments with SMX are apparently very influenced by the pH of the solution. Due to this, an adsorption study depending on the pH variation must be done, testing SMX in different matrices and concluding about the interference of pH in the adsorption of this drug.

The application of the produced activated carbons in a continuous operation mode, such as fixed-bed columns, can be explored, as well as scale-up tests using larger volumes of drug solution.

V. References

[1] O. A. H. Jones, N. Voulvoulis, and J. N. Lester, "Human harmaceuticals in wastewater treatment processes," *Crit. Rev. Environ. Sci. Technol.*, vol. 35, no. 4, pp. 401–427, 2005.

[2] B. Owens, "Pharmaceuticals in the environment: a growing problem," *Pharm. J.*, 2015.

[3] K. Kümmerer, "The presence of pharmaceuticals in the environment due to human use – present knowledge and future challenges," *J. Environ. Manage.*, vol. 90, no. 8, pp. 2354–2366, 2009.

[4] J. Rivera-Utrilla, M. Sánchez-Polo, M. Á. Ferro-García, G. Prados-Joya, and R. Ocampo-Pérez, "Pharmaceuticals as emerging contaminants and their removal from water: a review," *Chemosphere*, vol. 93, no. 7, pp. 1268–1287, 2013.

[5] V. Calisto, A. Bahlmann, R. J. Schneider, and V. I. Esteves, "Application of an ELISA to the quantification of carbamazepine in ground, surface and wastewaters and validation with LC–MS/MS," *Chemosphere*, vol. 84, no. 11, pp. 1708–1715, 2011.

[6] A. Bahlmann, J. J. Carvalho, M. G. Weller, U. Panne, and R. J. Schneider, "Immunoassays as high-throughput tools: Monitoring spatial and temporal variations of carbamazepine, caffeine and cetirizine in surface and wastewaters," *Chemosphere*, vol. 89, no. 11, pp. 1278–1286, 2012.

[7] A. Bahlmann, W. Brack, R. J. Schneider, and M. Krauss, "Carbamazepine and its metabolites in wastewater: Analytical pitfalls and occurrence in Germany and Portugal," *Water Res.*, vol. 57, pp. 104–114, 2014.

[8] R. C. Bansal and M. Goyal, *Activated carbon adsorption*. Taylor & Francis Group, 2005.

[9] I. Ali and V. K. Gupta, "Advances in water treatment by adsorption technology," *Nat. Protoc.*, vol. 1, no. 6, pp. 2661–2667, 2007.

[10] F. Rouquerol, J. Rouquerol, K. S. W. Sing, G. Maurin, and P. Llewellyn, *Adsorption by powders and porous solids*. Elsevier, 2014.

[11] W. J. Weber and J. C. Morris, "Kinetics of adsorption on carbon from solution," *J. Sanit. Eng. Div.*, vol. 89, no. 2, pp. 31–60, 1963.

[12] C. Moreno-Castilla, "Adsorption of organic molecules from aqueous solutions on carbon materials," *Carbon N. Y.*, vol. 42, no. 1, pp. 83–94, 2004.

[13] V. Calisto, C. I. A. Ferreira, J. A. B. P. Oliveira, M. Otero, and V. I. Esteves, "Adsorptive removal of pharmaceuticals from water by commercial and waste-based carbons," *J. Environ. Manage.*, vol. 152, pp. 83–90, 2015.

[14] R. Loos, B. M. Gawlik, G. Locoro, E. Rimaviciute, S. Contini, and G. Bidoglio, "EU-wide survey of polar organic persistent pollutants in European river waters," *Environ. Pollut.*, vol. 157, no. 2, pp. 561–568, Feb. 2009.

[15] K. Y. Foo and B. H. Hameed, "Insights into the modeling of adsorption isotherm systems," *Chem. Eng. J.*, vol. 156, no. 1, pp. 2–10, 2010.

[16] S. Brunauer, P. H. Emmett, and E. Teller, "Adsorption of gases in multimolecular layers," *J. Am. Chem. Soc.*, vol. 60, no. 2, pp. 309–319, 1938.

[17] C. H. Giles, T. H. MacEwan, S. N. Nakhwa, and D. Smith, "Studies in adsorption: A system of classification of solution adsorption isotherms, and its use in diagnosis of adsorption mechanisms and in measurement of specific surface areas of solids," *J. Chem. Soc.*, p. 3973, 1960.

[18] I. Langmuir, "The constitution and fundamental properties of solids and liquids," *J. Am. Chem. Soc.*, vol. 38, no. 11, pp. 2221–2295, 1916.

[19] K. R. Hall, L. C. Eagleton, A. Acrivos, and T. Vermeulen, "Pore- and solid-diffusion kinetics in fixed-bed adsorption under constant-pattern conditions," *Ind. Eng. Chem. Fundam.*, vol. 5, no. 2, pp. 212–223, 1966.

[20] H. Freundlich, "Over the adsorption in solution," vol. 57, no. 0. pp. 385–471, 1906.

[21] S. Lagergren, "About the theory of so-called adsorption of soluble substances," vol. 24, no. 4. pp. 1–39, 1898.

[22] Y. S. Ho, G. McKay, D. A. J. Wase, and C. F. Forster, "Study of the sorption of divalent metal ions on to peat," *Adsorpt. Sci. Technol.*, vol. 18, no. 7, pp. 639–650, 2000.

[23] S. H. Chien and W. R. Clayton, "Application of Elovich Equation to the Kinetics of Phosphate Release and Sorption in Soils1," *Soil Sci. Soc. Am. J.*, vol. 44, no. 2, p. 265, 1980.

[24] V. M. A. Calisto, "Environmental occurrence and fate of psychiatric pharmaceuticals," University of Aveiro, 2011.

[25] J. R. Glynn, B. M. Belongia, R. G. Arnold, K. L. Ogden, and J. C. Baygents, "Capillary electrophoresis measurements of electrophoretic mobility for colloidal particles of biological Interest," *Appl. Environ. Microbiol.*, vol. 64, no. 7, pp. 2572–7, 1998.

[26] L. Wei and G. Yushin, "Nanostructured activated carbons from natural precursors for electrical double layer capacitors," *Nano Energy*, vol. 1, no. 4, pp. 552–565, 2012.

[27] S. Babel, "Low-cost adsorbents for heavy metals uptake from contaminated water: a

review," *J. Hazard. Mater.*, vol. 97, no. 1–3, pp. 219–243, Feb. 2003.

[28] C. Saucier, M. A. Adebayo, E. C. Lima, R. Cataluña, P. S. Thue, L. D. T. Prola, M. J. Puchana-Rosero, F. M. Machado, F. A. Pavan, and G. L. Dotto, "Microwave-assisted activated carbon from cocoa shell as adsorbent for removal of sodium diclofenac and nimesulide from aqueous effluents," *J. Hazard. Mater.*, vol. 289, pp. 18–27, 2015.

[29] A. Jain, R. Balasubramanian, and M. P. Srinivasan, "Production of high surface area mesoporous activated carbons from waste biomass using hydrogen peroxide-mediated hydrothermal treatment for adsorption applications," *Chem. Eng. J.*, vol. 273, pp. 622–629, 2015.

[30] P. Nowicki, J. Kazmierczak, and R. Pietrzak, "Comparison of physicochemical and sorption properties of activated carbons prepared by physical and chemical activation of cherry stones," *Powder Technol.*, vol. 269, pp. 312–319, 2015.

[31] G. Z. Kyzas and E. A. Deliyanni, "Modified activated carbons from potato peels as green environmental-friendly adsorbents for the treatment of pharmaceutical effluents," *Chem. Eng. Res. Des.*, vol. 97, pp. 135–144, 2015.

[32] M. Antunes, V. I. Esteves, R. Guégan, J. S. Crespo, A. N. Fernandes, and M. Giovanela, "Removal of diclofenac sodium from aqueous solution by Isabel grape bagasse," *Chem. Eng. J.*, vol. 192, pp. 114–121, 2012.

[33] J. V. Flores-Cano, M. Sánchez-Polo, J. Messoud, I. Velo-Gala, R. Ocampo-Pérez, and J. Rivera-Utrilla, "Overall adsorption rate of metronidazole, dimetridazole and diatrizoate on activated carbons prepared from coffee residues and almond shells," *J. Environ. Manage.*, vol. 169, pp. 116–125, 2016.

[34] N. Ferrera-Lorenzo, E. Fuente, I. Suárez-Ruiz, and B. Ruiz, "KOH activated carbon from conventional and microwave heating system of a macroalgae waste from the Agar–Agar industry," *Fuel Process. Technol.*, vol. 121, pp. 25–31, 2014.

[35] T. Maneerung, J. Liew, Y. Dai, S. Kawi, C. Chong, and C.-H. Wang, "Activated carbon derived from carbon residue from biomass gasification and its application for dye adsorption: Kinetics, isotherms and thermodynamic studies," *Bioresour. Technol.*, vol. 200, pp. 350–359, 2016.

[36] G. Orlandi, J. Cavasotto, F. R. S. Machado, G. L. Colpani, J. D. Magro, F. Dalcanton, J. M. M. Mello, and M. A. Fiori, "An adsorbent with a high adsorption capacity obtained from the cellulose sludge of industrial residues," *Chemosphere*, vol. 169, pp. 171–180, 2017.

[37] T. L. Silva, A. Ronix, O. Pezoti, L. S. Souza, P. K. T. Leandro, K. C. Bedin, K. K. Beltrame, A. L. Cazetta, and V. C. Almeida, "Mesoporous activated carbon from industrial laundry sewage sludge: Adsorption studies of reactive dye Remazol Brilliant Blue R," *Chem. Eng. J.*, vol. 303, pp. 467–476, 2016.

[38] J. P. Kearns, L. S. Wellborn, R. S. Summers, and D. R. U. Knappe, "2,4-D adsorption to biochars: Effect of preparation conditions on equilibrium adsorption capacity and comparison with commercial activated carbon literature data," *Water Res.*, vol. 62, pp. 20–28, 2014.

[39] C. Djilani, R. Zaghdoudi, F. Djazi, B. Bouchekima, A. Lallam, A. Modarressi, and M. Rogalski, "Adsorption of dyes on activated carbon prepared from apricot stones and commercial activated carbon," *J. Taiwan Inst. Chem. Eng.*, vol. 53, pp. 112–121, 2015.

[40] C. I. A. Ferreira, V. Calisto, M. Otero, H. Nadais, and V. I. Esteves, "Comparative adsorption evaluation of biochars from paper mill sludge with commercial activated carbon for the removal of fish anaesthetics from water in Recirculating Aquaculture Systems," *Aquac. Eng.*, vol. 74, pp. 76–83, 2016.

[41] G. Jaria, V. Calisto, M. V. Gil, M. Otero, and V. I. Esteves, "Removal of fluoxetine from water by adsorbent materials produced from paper mill sludge," *J. Colloid Interface Sci.*, vol. 448, pp. 32–40, 2015.

[42] G. Jaria, C. P. Silva, C. I. A. Ferreira, M. Otero, and V. Calisto, "Sludge from paper mill effluent treatment as raw material to produce carbon adsorbents: An alternative waste management strategy," *J. Environ. Manage.*, vol. 188, pp. 203–211, 2017.

[43] N. Khalili, J. Vyas, W. Weangkaew, S. Westfall, S. Parulekar, and R. Sherwood, "Synthesis and characterization of activated carbon and bioactive adsorbent produced from paper mill sludge," *Sep. Purif. Technol.*, vol. 26, no. 2–3, pp. 295–304, 2002.

[44] W.-H. Li, Q.-Y. Yue, B.-Y. Gao, X.-J. Wang, Y.-F. Qi, Y.-Q. Zhao, and Y.-J. Li, "Preparation of sludge-based activated carbon made from paper mill sewage sludge by steam activation for dye wastewater treatment," *Desalination*, vol. 278, no. 1–3, pp. 179–185, 2011.

[45] V. Calisto, C. I. A. Ferreira, S. M. Santos, M. V. Gil, M. Otero, and V. I. Esteves, "Production of adsorbents by pyrolysis of paper mill sludge and application on the removal of citalopram from water," *Bioresour. Technol.*, vol. 166, pp. 335–344, 2014.

[46] M. C. Monte, E. Fuente, A. Blanco, and C. Negro, "Waste management from pulp and paper production in the European Union," *Waste Manag.*, vol. 29, no. 1, pp. 293–308,

2009.

[47] R. Azargohar and A. K. Dalai, “Steam and KOH activation of biochar: Experimental and modeling studies,” *Microporous Mesoporous Mater.*, vol. 110, no. 2–3, pp. 413–421, 2008.

[48] R. J. White, The search for functional porous carbons from sustainable precursors. 2015.

[49] H. Marsh and F. Reinoso-Rodríguez, *Activated carbon*. Elsevier Ltd, 2006.

[50] A. R. Yacob, Z. A. Majid, R. S. D. Dasril, and V. Inderan, “Comparison of various sources of high surface area carbon prepared by different types of activation,” *Malaysian J. Anal. Sci.*, vol. 12, no. 1, pp. 264–271, 2008.

[51] V. Calisto and V. I. Esteves, “Psychiatric pharmaceuticals in the environment,” *Chemosphere*, vol. 77, no. 10, pp. 1257–1274, 2009.

[52] M. Clara, B. Strenn, and N. Kreuzinger, “Carbamazepine as a possible anthropogenic marker in the aquatic environment: investigations on the behaviour of Carbamazepine in wastewater treatment and during groundwater infiltration,” *Water Res.*, vol. 38, no. 4, pp. 947–954, 2004.

[53] L. Yu, G. Fink, T. Wintgens, T. Melin, and T. A. Ternes, “Sorption behavior of potential organic wastewater indicators with soils,” *Water Res.*, vol. 43, no. 4, pp. 951–960, 2009.

[54] S. Á. Torrellas, R. García Lovera, N. Escalona, C. Sepúlveda, J. L. Sotelo, and J. García, “Chemical-activated carbons from peach stones for the adsorption of emerging contaminants in aqueous solutions,” *Chem. Eng. J.*, vol. 279, pp. 788–798, 2015.

[55] S. Larcher and V. Yargeau, “Biodegradation of sulfamethoxazole: current knowledge and perspectives,” *Appl. Microbiol. Biotechnol.*, vol. 96, no. 2, pp. 309–318, 2012.

[56] A. C. Johnson, V. Keller, E. Dumont, and J. P. Sumpter, “Assessing the concentrations and risks of toxicity from the antibiotics ciprofloxacin, sulfamethoxazole, trimethoprim and erythromycin in European rivers,” *Sci. Total Environ.*, vol. 511, pp. 747–755, 2015.

[57] E. Çalışkan and S. Göktürk, “Adsorption characteristics of sulfamethoxazole and metronidazole on activated carbon,” *Sep. Sci. Technol.*, vol. 45, no. 2, pp. 244–255, 2010.

[58] Y. Yao, B. Gao, H. Chen, L. Jiang, M. Inyang, A. R. Zimmerman, X. Cao, L. Yang, Y. Xue, and H. Li, “Adsorption of sulfamethoxazole on biochar and its impact on reclaimed water irrigation,” *J. Hazard. Mater.*, vol. 209–210, pp. 408–413, 2012.

[59] S. Teixeira, C. Delerue-Matos, and L. Santos, “Removal of sulfamethoxazole from

solution by raw and chemically treated walnut shells," *Environ. Sci. Pollut. Res.*, vol. 19, no. 8, pp. 3096–3106, 2012.

[60] G. Jaria, C. P. Silva, C. I. A. Ferreira, M. Otero, and V. Calisto, "Sludge from paper mill effluent treatment as raw material to produce carbon adsorbents: An alternative waste management strategy," *J. Environ. Manage.*, vol. 188, pp. 203–211, 2017.

[61] AENOR, Norma UNE 32002:1995.

[62] AENOR, Norma UNE 32019:1985.

[63] AENOR, Norma UNE 32004:1984.

[64] Y. Aldegs, M. Elbarghouthi, A. Elsheikh, and G. Walker, "Effect of solution pH, ionic strength, and temperature on adsorption behavior of reactive dyes on activated carbon," *Dye. Pigment.*, vol. 77, no. 1, pp. 16–23, 2008.

[65] H. P. Boehm, "Some aspects of the surface chemistry of carbon blacks and other carbons," *Carbon N. Y.*, vol. 32, no. 5, pp. 759–769, 1994.

[66] H. Marsh and B. Rand, "The characterization of microporous carbons by means of the dubinin-radushkevich equation," *J. Colloid Interface Sci.*, vol. 33, no. 1, pp. 101–116, May 1970.

[67] ICH, "Validation of analytical procedures: text and methodology," in *ICH Harmonised Tripartite Guideline*, 2005.

[68] H. Yang, R. Yan, H. Chen, D. H. Lee, and C. Zheng, "Characteristics of hemicellulose, cellulose and lignin pyrolysis," *Fuel*, vol. 86, no. 12–13, pp. 1781–1788, Aug. 2007.

[69] J. Coates, "Interpretation of Infrared Spectra, A Practical Approach," in *Encyclopedia of Analytical Chemistry*, Chichester, UK: John Wiley & Sons, Ltd, 2006.

[70] A. Ahmad, M. Loh, and J. Aziz, "Preparation and characterization of activated carbon from oil palm wood and its evaluation on Methylene blue adsorption," *Dye. Pigment.*, vol. 75, no. 2, pp. 263–272, 2007.

[71] A. Méndez, J. M. Fidalgo, F. Guerrero, and G. Gascó, "Characterization and pyrolysis behaviour of different paper mill waste materials," *J. Anal. Appl. Pyrolysis*, vol. 86, no. 1, pp. 66–73, Sep. 2009.

VI. Appendices

Appendix 1

Table 19 (Appendix 1) - SEM imagens of RP500, BP500, RP500-HCl and BP500-HCl at different magnitudes

M	RP500	BP500	RP500-HCl	BP500-HCl
300	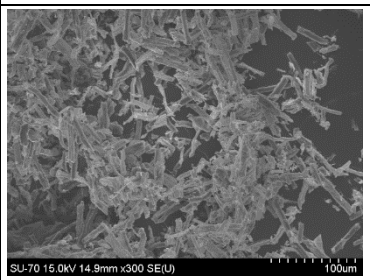	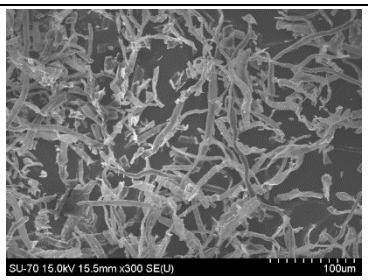	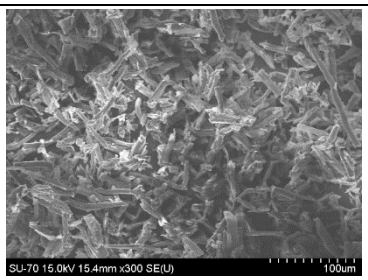	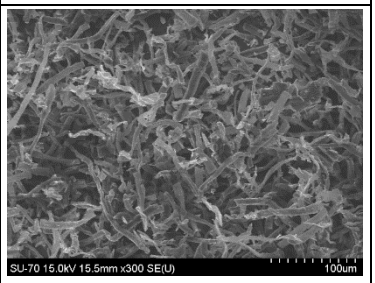
1K	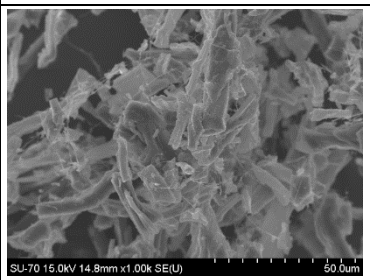	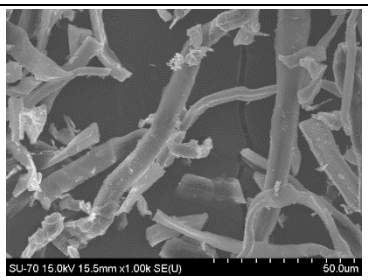	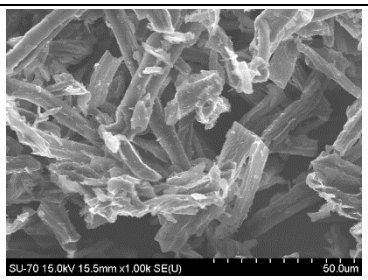	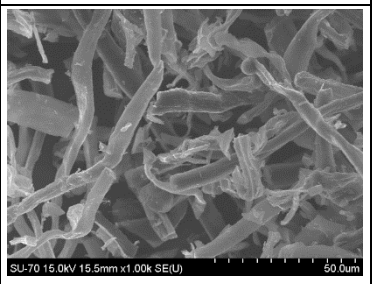
3K	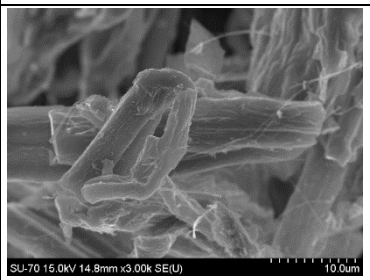	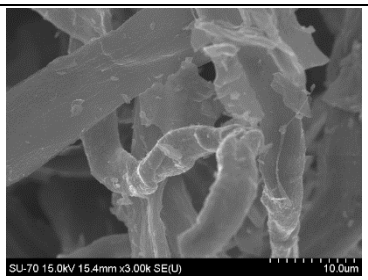	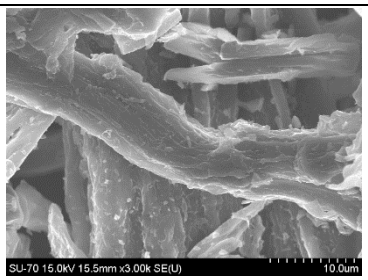	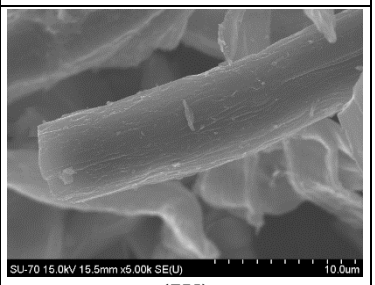 (5K)
10K	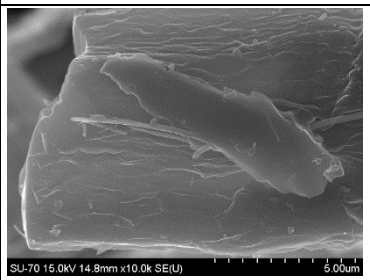	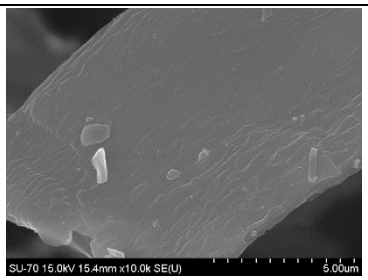	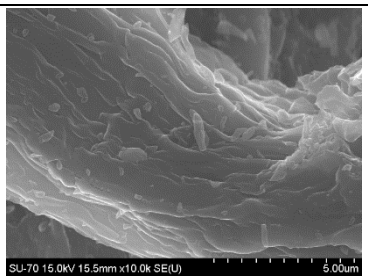	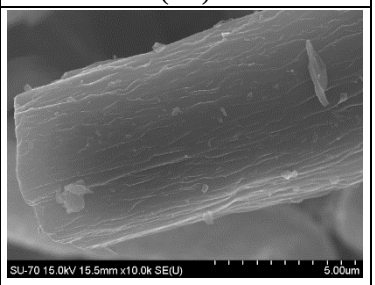
30K	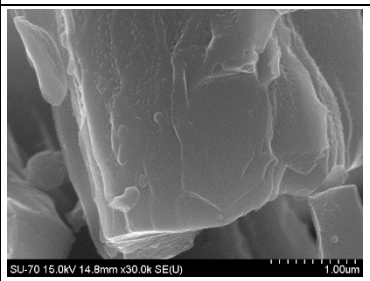	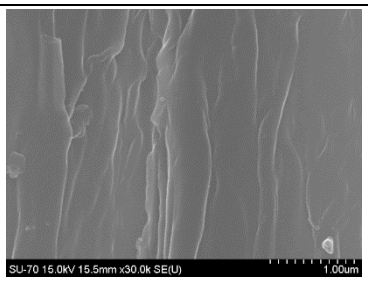	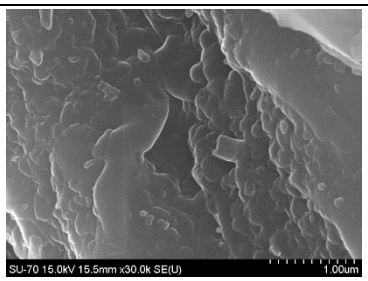	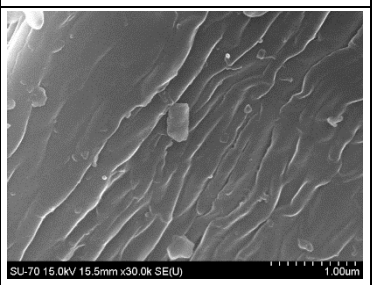

Legend: M – Magnitude; K – $x10^3$

Table 20 (Appendix 1) - SEM imagens of RP800, BP800, RP800-HCl and BP800-HCl at different magnitudes

M	RP800	BP800	RP800-HCl	BP800-HCl
300	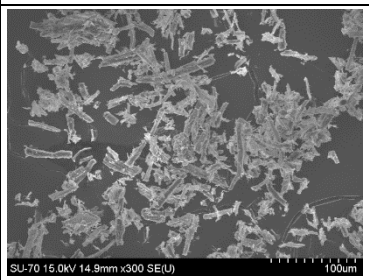	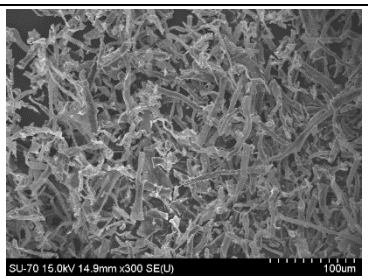	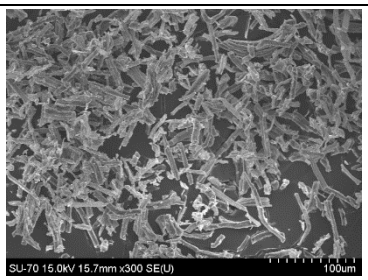	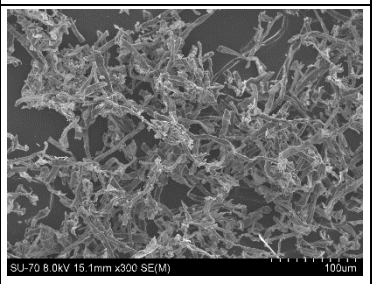
1K	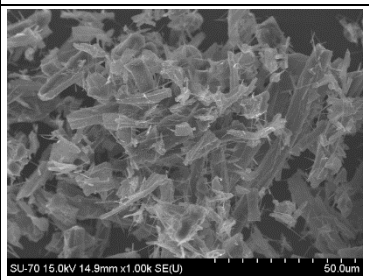	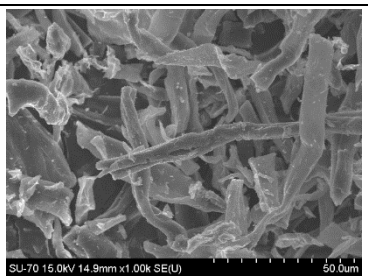	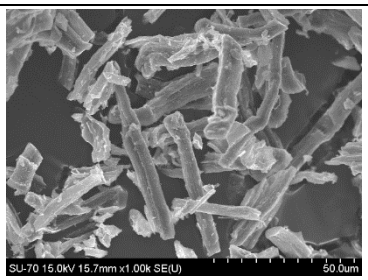	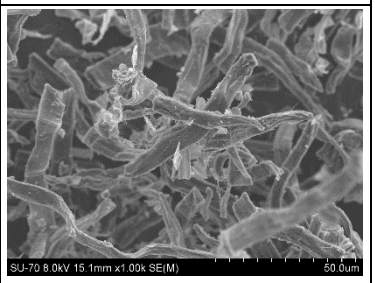
3K	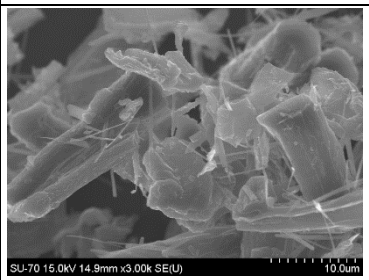	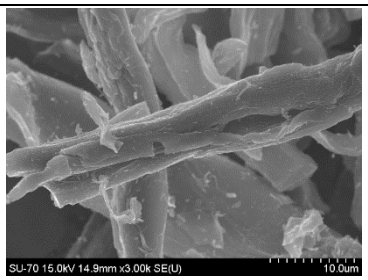	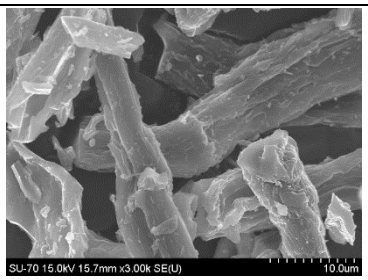	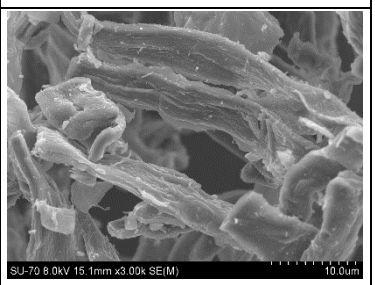
10K	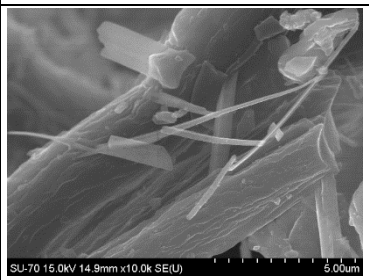	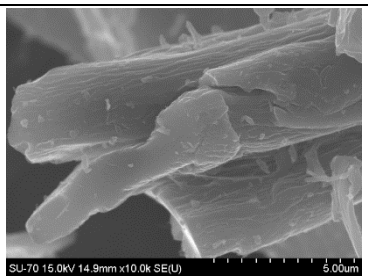	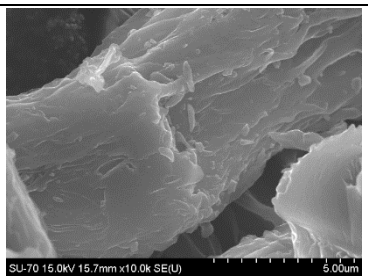	
30K	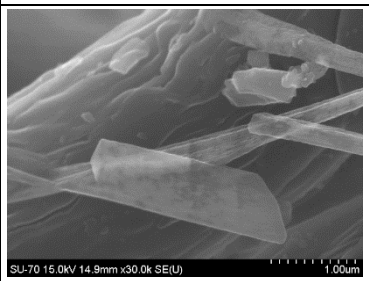	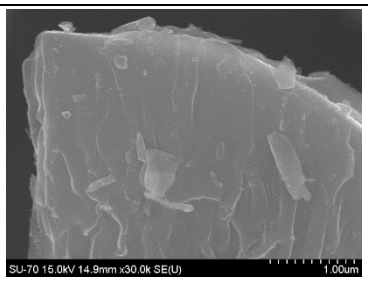	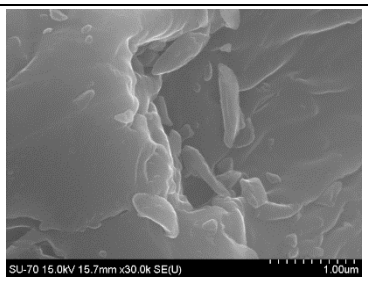	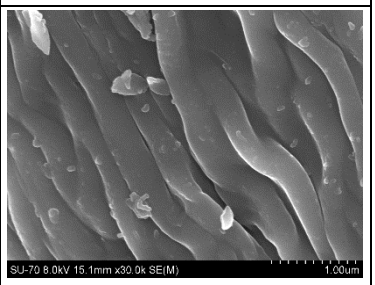
Legend: M – Magnitude; K – $x10^3$				

Table 21 (Appendix 1) - SEM imagens of all activated carbons at different magnitudes

M	**RP800-HCl-K_2CO_3**	**BP800-HCl-K_2CO_3**	**RP800-HCl-H_3PO_4**	**BP800-HCl-H_3PO_4**
300	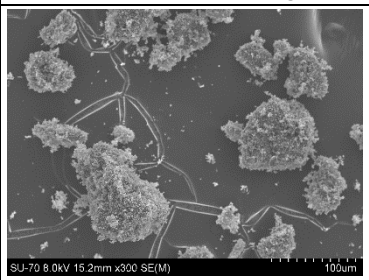	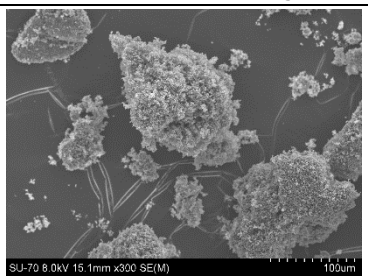	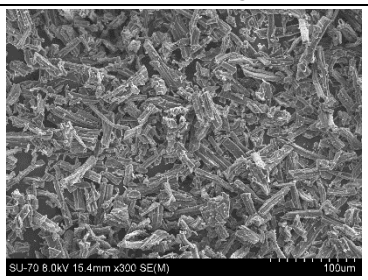	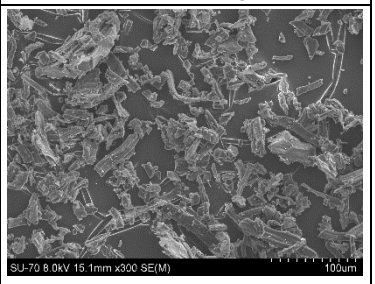
1K	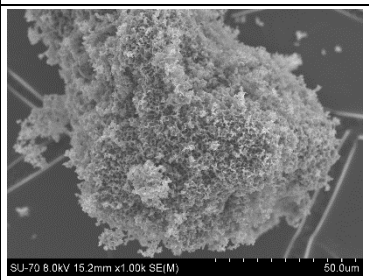	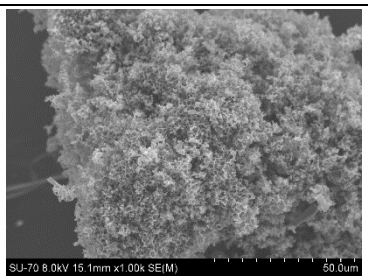	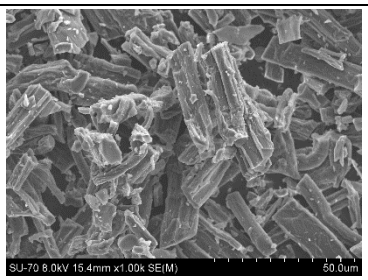	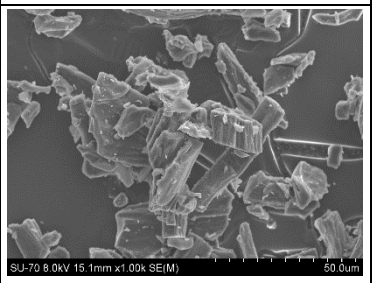
3K	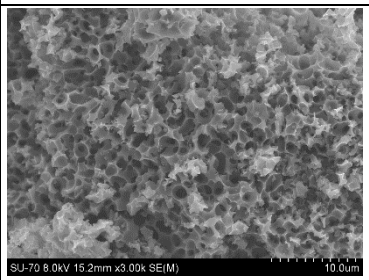	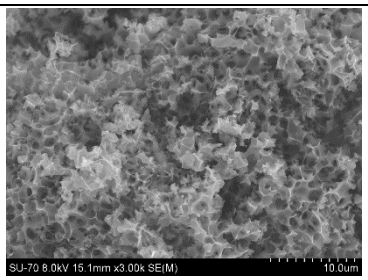	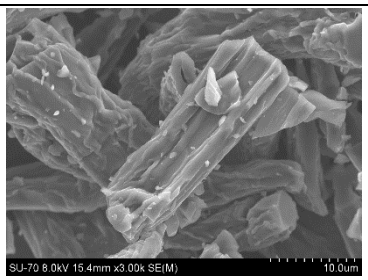	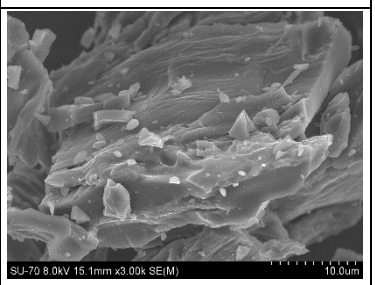
10K	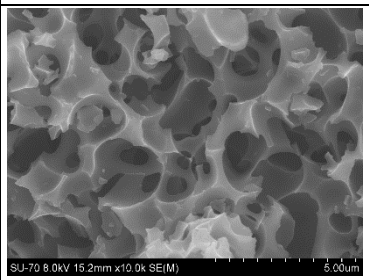		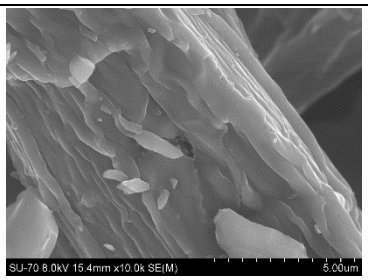	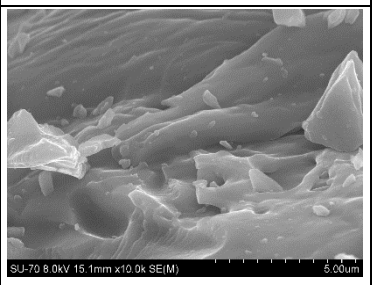
30K	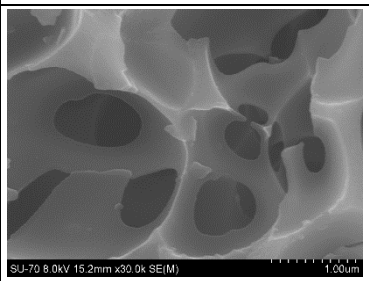	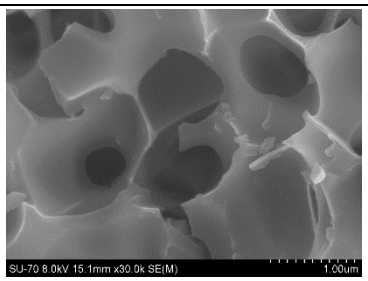	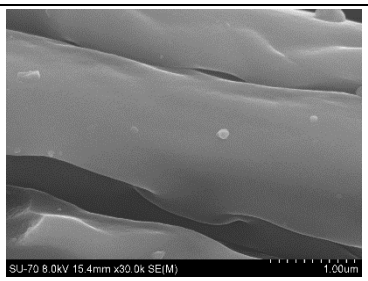	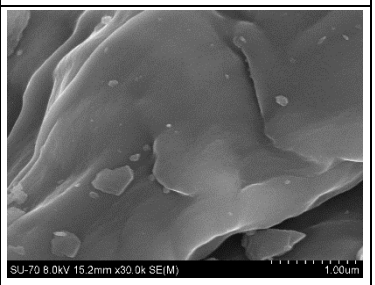
Legend: M – Magnitude; K – $x10^3$				

Table 22 (Appendix 1) - SEM imagens of RP and BP at different magnitudes

M	**RP**	**BP**
300	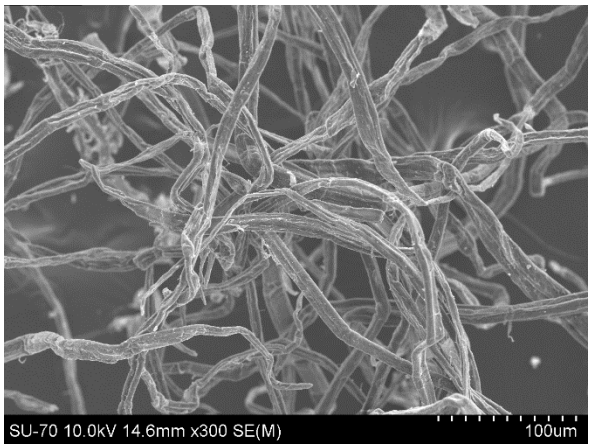	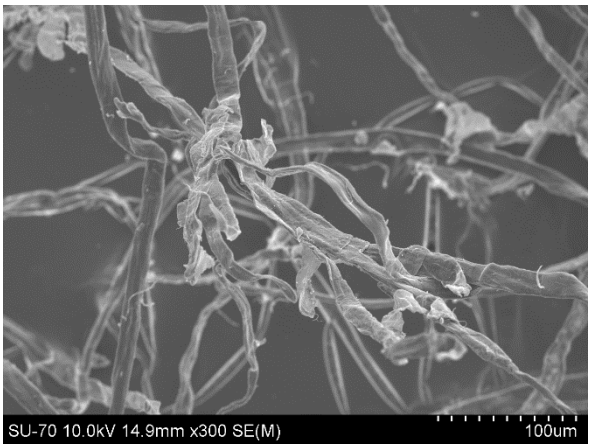
3K	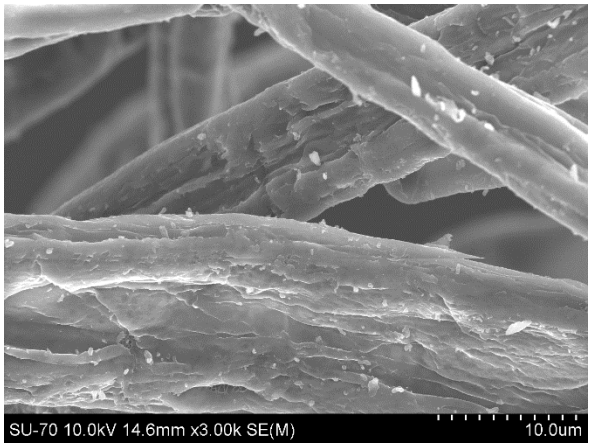	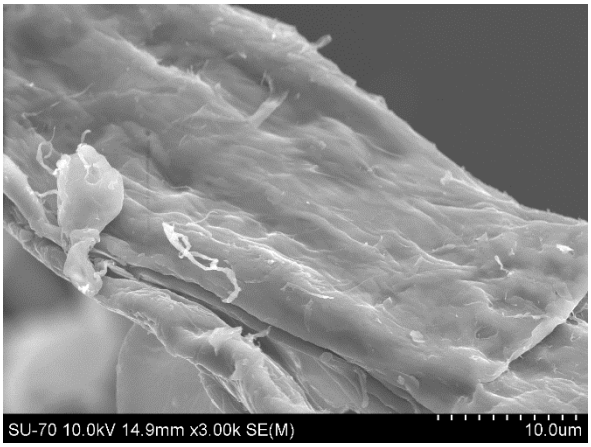
10K	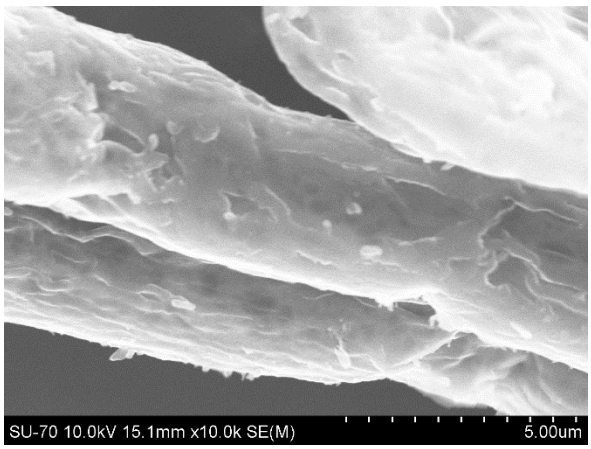	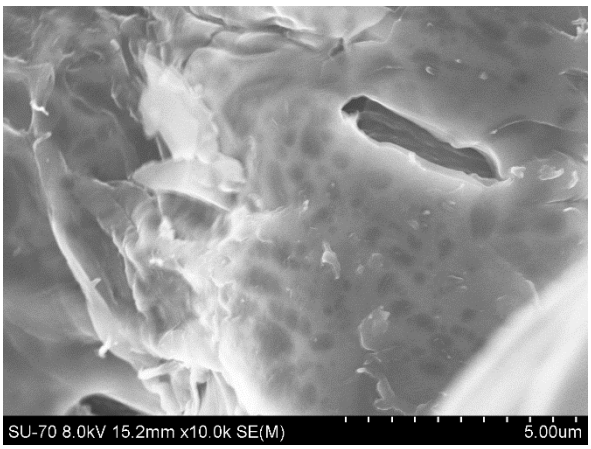
Legend: M – Magnitude; K – $x10^3$		

Appendix 2

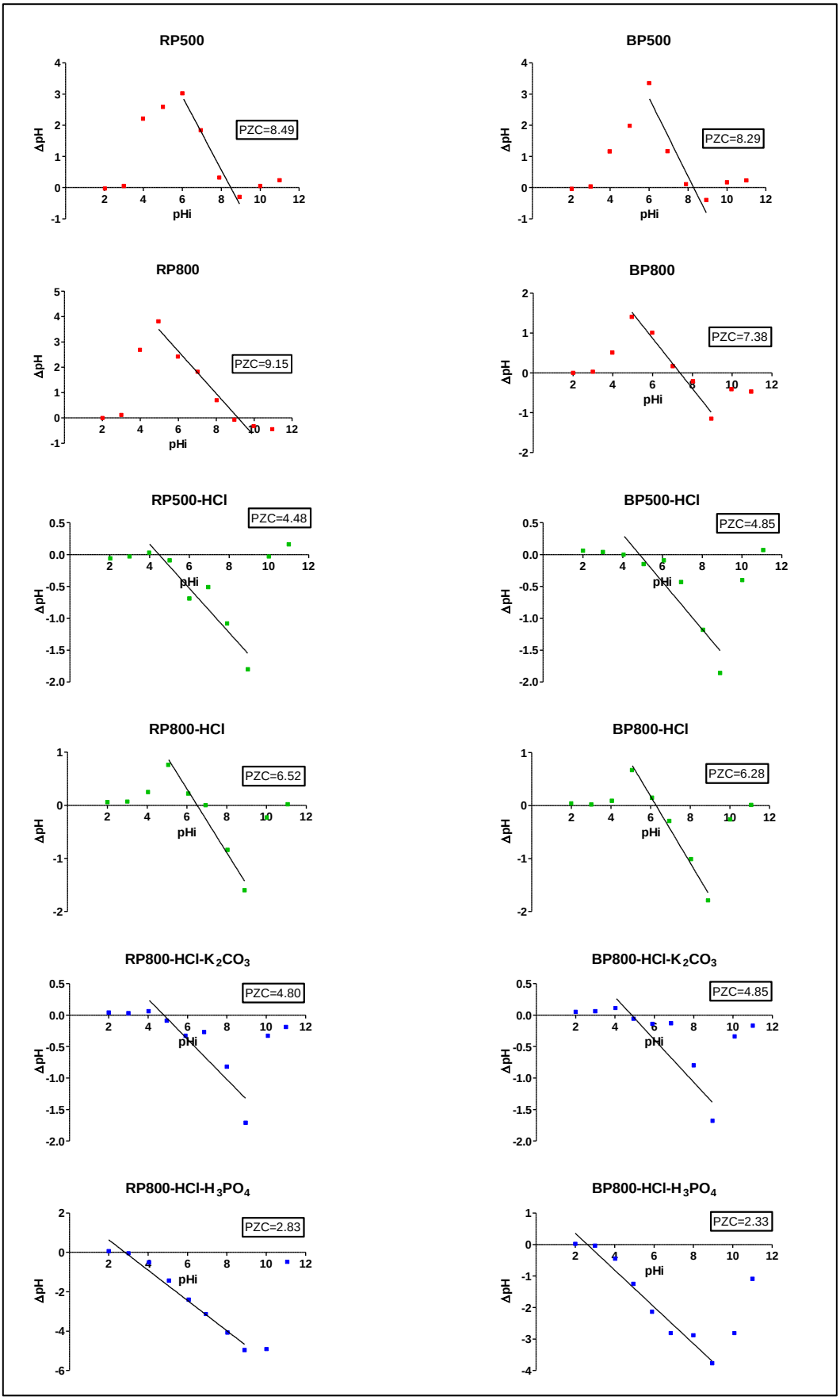

Figure 19 (Appendix 2) - PZC graphs of all produced carbons